A Computational Investigation of Myelination and Epilepsy

Odin Dumas

Thesis Submitted to the University of Ottawa in
Partial Fulfillment of the Requirements for
the Degree of Master of Biology

Department of Biology
Faculty of Science
University of Ottawa

Contents

Statement of Contribution

The completion of this Master's thesis in computational neuroscience has been significantly bolstered by the invaluable contributions and guidance provided by esteemed colleagues and experts in the field.

I would like to express my profound gratitude to my supervisor, Dr. Jérémie Lefebvre, whose unwavering support and insightful guidance were instrumental in shaping the direction and depth of this research. Dr. Lefebvre's expertise in computational modeling and theoretical neuroscience provided the foundational framework upon which this thesis was built. The thalamocortical network informed by Wilson-Cowan equations built by Dr. Lefebvre was essential in our investigations of ADM and seizure progression. His critical feedback and encouragement fostered a rigorous and thorough approach to the research questions addressed herein.

Additionally, I extend my sincere appreciation to Dr. Juliet Knowles and her laboratory team for their pivotal role in the experimental validation of our computational model. The empirical data and results obtained from Dr. Knowles' lab were crucial in validating the theoretical constructs and simulations presented, particularly in Chapter 3 of this thesis. Their collaborative efforts not only enriched the scientific rigor of this work but also ensured its relevance and applicability to real-world neurobiological phenomena. The real-world applicability then allowed further investigations using computational models that provided insights regarding issues that may be difficult or time-consuming to implement experimentally.

I would also like to thank Dr. Scott Rich, whose research on neural heterogeneity I recreated as a way to familiarize myself with the models I would use throughout my thesis. This initial work provided a solid foundation for our models, and greatly facilitated my understanding and application of the computational techniques employed in this research.

This thesis is a testament to the collaborative nature of scientific research, demonstrating the synergy between computational predictions and experimental findings. The combined expertise of Dr. Lefebvre, Dr. Knowles, and Dr. Rich significantly enhanced the scope and impact of this research, contributing to a deeper understanding of the complex dynamics underlying neural systems.

I am deeply grateful for their contributions, which were indispensable to the successful completion of this work.

Abstract

Epilepsy, characterized by recurrent seizures, is one of the most prevalent neurological diseases worldwide [1]. Recent advances suggest that myelination, the insulating sheaths around axons of neurons, plays a crucial role in the neuronal network's functionality and might influence epilepsy [2]. This thesis explores the relationship between myelination and the dynamics of epilepsy through computational modeling, specifically with the Wilson-Cowan model, a well-established framework for understanding interactions within neural populations. We modified the traditional Wilson-Cowan equations to incorporate variables representing myelination and conducted simulations to observe how changes in myelination affect seizure activity in neural networks. The results indicate that increases in myelination along specific tracts can significantly alter the excitatory and inhibitory dynamics of neural populations, leading to increased seizure burden. These findings could provide new insights into epilepsy management and suggest myelination as a target for novel therapeutics. This study not only enhances our understanding of epilepsy's pathophysiology but also underscores the importance of myelination in neural circuits and disease progression.

L'épilepsie, caractérisée par des crises récurrentes, est l'une des maladies neurologiques les plus prévalentes dans le monde [1]. Des avancées récentes suggèrent que la myélinisation, les gaines isolantes autour des axones des neurones, joue un rôle crucial dans la fonctionnalité du réseau neuronal et pourrait influencer l'épilepsie [2]. Cette thèse explore la relation entre la myélinisation et la dynamique de l'épilepsie à travers la modélisation computationnelle, spécifiquement avec le modèle de Wilson-Cowan, un cadre bien établi pour comprendre les interactions au sein des populations neuronales. Nous avons modifié les équations traditionnelles de Wilson-Cowan pour incorporer des variables représentant la myélinisation et avons mené des simulations pour observer comment les changements dans la myélinisation affectent l'activité des crises dans les réseaux neuronaux. Les résultats indiquent que les augmentations de la myélinisation le long de tracts spécifiques peuvent modifier significativement les dynamiques excitatrices et inhibitrices des populations neuronales, conduisant à une augmentation du fardeau des crises. Ces découvertes pourraient offrir de nouvelles perspectives dans la gestion de l'épilepsie et suggèrent la myélinisation comme cible pour de nouveaux traitements thérapeutiques. Cette étude améliore non seulement notre compréhension de la physiopathologie de l'épilepsie, mais souligne également l'importance de la myélinisation dans les circuits neuronaux et la progression de la maladie.

Acknowledgements

I would like to thank everyone who supported me during the writing of this thesis. Special thanks to Dr. Jérémie Lefebvre, my supervisor, for his invaluable guidance and support. I am also very grateful to my lab mates who were always willing to lend a helping hand, as well as Dr. Juliet Knowles and her lab for providing biological data sets that would guide my thesis.

List of Figures

List of Tables

Chapter 1

Introduction

1.1 Chapter Summary

In this chapter we give an overview of epilepsy, delineating between subtypes relevant to the ensuing research. We then move on to understanding which neuron types are present, as well as how they function within the constraints of computational models. Next we describe the motivation for this research, looking at recent developments that have put forth myelination as an important pathological factor in certain forms of epilepsy. This is followed up by a holistic discussion of Wilson-Cowan models, which are a class of computational models used to represent and investigate neural activity. We then describe some of the methods used in our research to quantify neural activity, which allow us to draw conclusions based on given sets of data. Lastly, we use the Wilson-Cowan models to investigate heterogeneity as it relates to epilepsy, in order to give a taste of what these models are capable of, as well as to reproduce previous results in our lab from Dr. Jeremie Lefebvre and Dr. Scott Rich [3].

1.2 Neurophysiology of a Neuron

While there are many different types of neurons that have many different roles and functions, most neurons share a set of common characteristics. One being dendrites, which are the branching structures that receive external input and transport that input to the soma [4]. The soma, also known as the cell body, integrates all of the dendritic input and can propagate its own action potential based on the summed membrane potential inputs from its dendrites. If threshold conditions are met, the soma will send the action potential down along its axon, which is like a cable that connects this neuron to other neurons, allowing it to affect their activity by synapsing onto their dendrites. The effect one neuron has on another is heavily dependent on its subtype. Two of the most common subtypes in the brain are the excitatory pyramidal neuron, and the inhibitory interneuron [5] [6]. As evidenced by the name, the excitatory pyramidal neuron serves to increase the likelihood of firing by downstream neurons, whereas the inhibitory interneuron serves the opposite function.

Practically, the action potential is passed between neurons through chemical synapses

using neurotransmitters, which are released by a presynaptic neuron and have either an excitatory or inhibitory effect on the postsynaptic neuron. The type of neurotransmitter depends on the presynaptic neuron, for example, pyramidal neurons release glutamate which is an excitatory neurotransmitter, thus increasing the likelihood of action potential propagation to its postsynaptic counterpart. Importantly, in order to trigger action potentials in the postsynaptic cell, numerous excitatory potentials must work together in a short time frame to create sufficient depolarization [7]. Inhibitory interneurons, on the other hand, release GABA, which reduces the likelihood of action potential propagation in the postsynaptic neuron. Overall, while there are many neuronal subtypes in the brain, these two provide a solid basis for understanding the activity between and amongst excitatory and inhibitory neurons.

1.3 What is Epilepsy?

Pathologies

Epilepsy is a disease defined by recurrent seizures with a number of different pathologies and symptoms. In Canada epilepsy affects approximately 4 out of every 1000 people, making it one of the most common serious neurological disorder in the country [8]. It becomes of further concern when quality of life measures are taken into consideration, as those afflicted are more than twice as likely to experience mood disorders, as well as more than eight times as likely to experience incontinence [8]. Overall, the disease is one characterized by hypersynchronous dynamics within the brain, where certain factors can allow for easier transitions to hypersynchronous states, resulting in these recurring seizures [9]. It is important to note the difference between seizure activity and epilepsy. While all individuals who have epilepsy must experience seizures in order to be diagnosed, it is possible for those who suffer from a seizure event to not be epileptic, as other factors exist that may induce seizure activity [1]. There are many types of seizures, however the two most common are focal and generalized.

Focal seizures, as the name suggests, arise in a specific area of the brain, and are often caused by brain lesions which can result from brain trauma [10]. While a focal zone can be larger or smaller than a single cortical area, seizures are restricted to a single hemisphere at onset. One common example is temporal lobe epilepsy, where seizure onset occurs in the medial temporal lobe, often due to trauma induced brain lesions [11]. Alternative to these focal types, generalized seizures can occur in both hemispheres of the brain simultaneously and often present bilateral motor symptoms. Important subtypes of generalized epilepsy's include idiopathic generalized epilepsy (IGE), which occurs without a consistent onset zone [12]. Although focal seizures can spread after onset, causing bihemispheric seizure activity, distinguishing focal from generalized pathologies is essential as it dictates the types of treatments available, as well as the types and severity of symptoms likely to arise [13].

Absence seizures are a subtype characterized by a lack of motor symptoms, and can act as a precursor to generalized forms of epilepsy, including IGEs. Often seen in progressive forms of childhood epilepsy, absence seizures act as a marker for pathologies that could be targeted with the goal of mitigating progression in order to reduce long term impact on patients [12] [14].

Etiology of Epilepsy

An important underlying hypothesis in epileptogenesis is the balance between excitation and inhibition (E-I) [15] [16] [17]. Much of the early research in epilepsy centered around hyperexcitability in cortical areas caused by overactive excitatory populations and/or underactive inhibitory populations. While this pathophysiological mechanism is relevant in many seizure types, there are many others that arise due to upregulated inhibition. This increased inhibition can also drive hypersynchronous activity with or without the help of overactive excitatory populations. An example of this imbalance is illustrated in the Scn8a mouse model, where it has been shown that mice with a loss of function mutation in the voltage gated sodium channel gene Scn8a can have recurrent connections in their reticular thalamic

nucleus (RTN) disturbed [18]. The RTN is an inhibitory neuron population that acts as a suppressor of hypersynchrony in cortical areas; mutations in the Scn8a gene inducing loss of function in these inhibitory neurons also cause a loss of suppressor function [19]. Once suppression is inhibited through hypo-inhibition, absence seizures are known to spontaneously arise, with the ability to generalize to other cortical areas [18] [20]. Another contributing factor in epilepsy pathology is heterogeneity of these cell types, which has been shown to influence the propensity for seizure activity, where greater neural diversity has a protective effect against the spread of hyperactivity, similar to many natural phenomena [3] [21]. Overall, different schemes of E-I imbalances can act alone, or together, in order to generate numerous seizure subtypes, whether they be generalized, focal, or other [22].

In order to give a holistic view of seizure events, we must also discuss the manifestation. Some manifestations include the ictal phase, tonic and clonic movements, along with oscillatory frequency of electrical activity in the brain, which can be picked up by electroencephalogram (EEG) recordings [23]. The ictal phase is defined as the phase in which a seizure event occurs, and is indicated by onset of epilepsy related symptoms. These symptoms include changes in level of consciousness, abnormal sensations, as well as involuntary muscle contractions [24]. It is important to note that symptoms vary greatly depending on the type of epilepsy, as well as the specific cortical areas afflicted by the hyperoscillatory activity. The clinical symptoms along with EEG analysis allow for proper diagnoses, where electrical activity within the brain gives clues as to the point of origination, as well as potential manifestations of the pathological oscillations. Among these manifestations are the well known tonic and clonic movements, which are characterized by muscle stiffening and rhythmic jerking of muscles respectively [25]. Some seizures, known as tonic-clonic seizures, can show both tonic and clonic activity, and are of the most recognizable yet debilitating group of seizure events [26].

Seizure Dynamics

The importance of EEGs in seizure diagnosis cannot be understated, specifically due to its ability to elucidate oscillatory frequencies which have pathological implications [27]. There is a lot of variance in terms of the frequencies involved in seizure events, where frequency bands such as delta (1-4 Hz), theta (4-8 Hz), alpha (8-12 Hz), beta (12-30 Hz), and gamma (above 30 Hz) have all been observed in different EEG recordings of seizure events [28]. From these bands however, we gain insight into the specific functions and dysfunctions occurring during the seizure event. For example, fast gamma activity has been implicated with the preictal phase, indicating the onset of a seizure, whereas slower delta oscillations may imply the postictal recovery period [29] [30]. The frequencies also allow us to delineate between seizure types as well as localize their point of origin, where focal seizures, originating in a specific cortical area often show high-frequency activity, whereas generalized seizures which originate in both hemispheres at onset tend to show a greater variety of frequency bands [31] [32].

Seizure dynamics result from the combination of abnormal membrane potential fluctuations in individual neurons, along with complex physiological disturbances at the level of populations of cells occurring during a seizure event.

These dynamics also vary depending on seizure types (i.e., focal, absence seizures). Focal Seizures, for example, originate in one specific area of the brain and typically present with symptoms indicating an onset, as well as varying levels of consciousness [33]. Absence Seizures, on the other hand, are characterized by their brief and sudden onset, typically involving a blank stare and a lack of awareness of the surrounding environment. These episodes are usually brief, lasting only a few seconds, but can occur frequently throughout the day, often impacting attention and daily activities [34].

In order to properly grasp the full scope of these events, we must understand their characteristics. Oftentimes, the phases of a focal seizure present in one of two primary patterns on an EEG. These patterns are low-voltage fast (LVF) and hypersynchronous (HYP) onsets, each of which is associated with specific neural dynamics [17]. Pre-ictal activity

typically lacks distinct features on the EEG, making it difficult to track from a clinical perspective. However, as a seizure begins, LVF onset presents with low-amplitude fast oscillations in the gamma spiking frequency range, and is often marked with a sentinel spike along with extremely high frequency oscillations in the range of 80-200Hz, which is a marker of its tonic phase. Alternatively, HYP onset can be characterized by its initial high amplitude spikes oscillating with a frequency of 1Hz, which suggest more focal onsets and is a pre-ictal marker. HYP is associated with extremely high frequency oscillations as well, with them being in the range of 250-500Hz, occuring during the tonic phase. Both described patterns can evolve into consistent oscillatory activity, transitioning from tonic to clonic phases, where oscillatory frequency then decreases until hypersynchronous dynamics are no longer present [17]. The tonic phase is characterized by continuous, high-frequency neuronal firing leading to sustained muscle contractions, while the clonic phase involves intermittent, synchronized bursts of neuronal activity causing rhythmic jerking movements. These phases reflect the changes in brain electrical activity during a seizure, highlighting the shift in balance between excitatory and inhibitory neural signals. Absence seizures however, are characterized by brief, sudden lapses in consciousness that typically last for a few seconds. Unlike focal seizures, absence seizures have a very abrupt onset and resolution, with the individual usually resuming their previous activity without any postictal confusion. The underlying neural dynamics involve a synchronized oscillatory activity between the thalamus and cortex, primarily mediated by T-type calcium channels [35]. These seizures do not exhibit the tonic-clonic phases seen in other seizure types but instead display a consistent spike-and-wave pattern throughout their duration [36].

Examples of these distinct subtypes are in Figure 1, where computational EEG data illustrates a focal seizure in Figure 1A, and recordings within the somatosensory cortical areas of mice show an absence seizure oscillating at approximately 8Hz in Figure 1 B, which is on the edge of theta and alpha band activity. Focal seizures, shown in Figure 1A/B, are specific to one area of the brain at onset, and oscillate at much higher frequencies relative

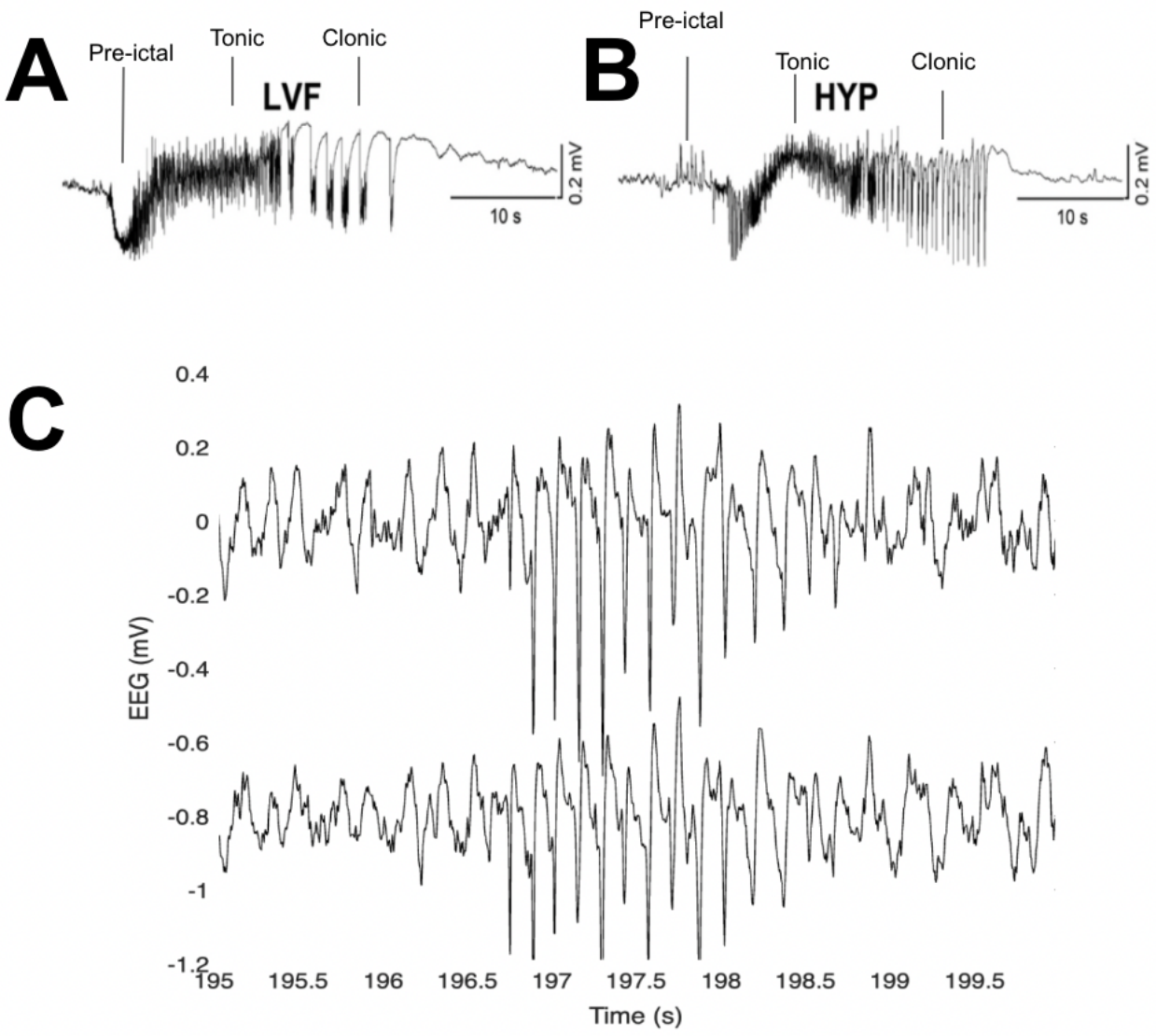

Figure 1: **EEG recordings of focal and absence seizures in and animal models**

(A) Human EEG recording of low-voltage fast (LVF) seizure onset, illustrating focal seizure dynamics shifting from pre-ictal activity, to fast tonic oscillations then to clonic activity. (B) Human EEG recording of hypersynchronous (HYP) seizure onset, also illustrating focal seizure dynamics with pre-ictal, tonic, and clonic phases defined, however with oscillations at different frequencies. (C) EEG recording of Scn8a KO mouse model depicting an absence seizure occurring over the course of 5 seconds in a thalamocortical network. Each trace represents a population (excitatory or inhibitory) in one hemisphere. Absence seizure data is provided by our collaborators (Knowles Lab, Stanford), and focal seizure data is provided in [17].

to absence seizures. We will focus primarily on this subtype in Chapter 2, where local E-I networks will be investigated for their susceptibility to seizure dynamics with respect to myelination. Absence seizures in bihemispheric networks, which will be further investigated in Chapter 3, are a seizure subtype specifically implicated in myelin associated progressive forms of the disease, often characterized by a sudden onset in both hemispheres, thus giving it a generalized pathology [2]. Furthermore, the abnormal neural activity of absence seizures typically originates in thalamocortical loops, and is hypothesized to be caused by alternating phase locked activity of GABAergic inhibition and glutamatergic excitation [37]. Overall, by understanding the different dynamics at play such as the ictal phases, tonic and clonic movements, frequency bands, we are able to diagnose and better understand the pathophysiological mechanisms at play, leading to better outcomes in clinical settings.

1.4 Myelination as a Pathology for Epilepsy Progression

There are a number of focal areas in epilepsy research, however up until recently, myelination has flown well under the radar. As it turns out, myelination patterns heavily influence ictal activity, including onset and progression of the disease as a whole [2]. Myelin itself is a fatty tissue that serves the function of insulating nerve fibers, and allowing for saltatory conduction along the axon, which in turn sees neural signals to jump between gaps in myelin, increasing speed and efficiency of transmission [38]. Thickness of myelin surrounding axons influences the conduction velocity (CV) of travelling action potentials, and is quantified by the g-ratio. G-ratio is a measure of myelin thickness relative to axonal width, whereby one divides axonal diameter by the diameter of the fiber [2]. A lower g-ratio thus indicates a relatively more myelinated tract which will thus have a higher CV. Additionally, myelin possesses the ability to align signals from different regions in time, as increased myelination of a longer tract could offset the greater distance action potentials must travel, allowing incidental arrival of two signals on a postsynaptic target.

It is important to understand that myelin is a plastic part of human physiology. Differ-

ent environmental factors can alter myelination patterns in the brain over time, one being activity dependent myelination [39]. For example, relatively high usage of a given neuronal tract may reduce g-ratio, as activity will stimulate oligodendrocyte progenitors to differentiate into mature oligodendrocytes, resulting in increased CV along the axon [40] [41]. Activity-dependent myelination (ADM) is heavily implicated in important neural processes, where MRI recordings have shown white matter plasticity along specific tracts in response to learning, and memory impaired mice show significant improvement to increased myelination in the hippocampus [42] [43] [2]. ADM becomes of great interest when studying epilepsy, as an increase in myelination could allow different cortical regions to synchronize more easily, uncovering another potential pathology for the disease. This specific pathophysiological mechanism was studied in mouse models, and results illustrated the interplay between seizure activity and epilepsy progression [2]. It was shown that absence seizures in a specific network stimulated oligodendrogenesis and myelination of said network as a direct result, lowering g-ratio and leaving more heavily myelinated axons, allowing faster communication [2]. The hypermyelination resulting from hyperactivity of absence seizures becomes more problematic when its effect is taken into consideration. It has been shown that faster communication in a seizure prone network, or any neural network for that matter, can induce hypersynchronous dynamics leading to stronger and more frequent seizures. This schema is exactly what is observed in Scn8a mouse models, where a positive feedback loop between seizure activity and induced myelination causes more seizures, thus further myelinating the network [2]. Interplay between ADM and epilepsy has thus become a central component in understanding epilepsy. Myelination as a pathology is especially exciting for types of epilepsy characterized by onset and quick progression, especially progressive childhood types, as they have historically been unresponsive to medication [44]. This new mechanism, however, provides novel ways to target the disease, and early experiments in mouse and rat models have illustrated a reduction of epilepsy progression through blocking ADM [2]. Furthermore, certain treatments coincidentally influencing ADM have had some limited success in mitigating disease

severity in progressive cases [2]. Overall, this new understanding of myelination as a contributing factor towards epilepsy pathology provides exciting avenues for future research and treatments.

1.5 The Wilson-Cowan Model

Background

It is quite a task to create physiologically accurate computational models of neural activity, and even more so of diseased brain states. However, computational methods can lend guidance to future experimentation and be compared to animal models in order to verify experimental methods. A variety of different models have been constructed over the past decades, some more biological, others more phenomenological [45]. The Wilson-Cowan model represents a powerful albeit phenomenological framework, that can be constrained by biological parameters, to emulate electrophysiological data that resembles in vivo recordings, and that can be modulated to gain insight into mechanisms underlying neural dynamics, notably epilepsy [46] [47]. In broad strokes, the Wilson-Cowan model is fairly intuitive: two neuron populations, excitatory pyramidal cells and inhibitory interneurons, interact to form a network. The activity of cells in each of these populations are represented by their mean, and both have recurrent connections, amongst and between them. It is important to note that Wilson-Cowan equations create a mean-field type model, where physiological relevance is balanced with computational tractability. This balance allows for a macroscopic view of neural activity amenable to examine interactions between cortical regions, which is advantageous when investigating epilepsy and cortical networks [48].

This model represents cortical network motifs at a local scale, such as in the somatosensory cortex, for instance. Neuronal micro columns in these areas consist of highly correlated neurons, enabling their collective electrical activity to be represented by a single mean activity. This simplifies the creation of a macroscopic view of neural activity, making interpre-

tation easier [49].

Once visualized in Figure 2, the model becomes fairly intuitive, and using the Wilson-Cowan formalism, many other neural properties and dynamics can be reproduced and investigated. Seizure-like dynamics emerge naturally in the Wilson-Cowan model in the form of abrupt, sudden transitions from asynchronous to oscillatory activity resulting from increased recruitment of excitatory/inhibitory populations (e.g. stimuli or input) [3] [50]. The mechanism responsible for these sudden transitions is linked to bifurcations, in which the system undergoes a both qualitative and quantitative regime shift, commonly leading to multistability [51]. Parameters of the Wilson-Cowan model may also be tuned to reproduce key dynamical and spectral features commonly observed during seizures, making it a great tool to use in our research [17] [52].

Mathematical Representation

Mathematically, the Wilson-Cowan formalism describes the dynamics of the mean membrane potentials of excitatory pyramidal (PYR), and inhibitory interneuronal (IN) populations through the following set of stochastic differential equations:

$$\alpha_{PYR}^{-1}\frac{dV_{PYR}}{dt} = -V_{PYR} + W_{PYRPYR}\cdot f\left[V_{PYR}\right] + W_{INPYR}\cdot f\left[V_{IN}\right] + \sqrt{2D}\xi_{PYR}(t) \qquad (1)$$

$$\alpha_{IN}^{-1}\frac{dV_{IN}}{dt} = -V_{IN} + W_{ININ}\cdot f\left[V_{IN}\right] + W_{PYRIN}\cdot f\left[V_{PYR}\right] + \sqrt{2D}\xi_{IN}(t) \qquad (2)$$

where V_{PYR} and V_{IN} represent the mean somatic membrane potentials of excitatory and inhibitory populations respectively. The parameter α_{PYR}^{-1} refers to the excitatory rate constant of 100Hz and α_{IN}^{-1} is the inhibitory rate constant of 200Hz. The inhibitory rate constant is greater than its excitatory counterpart due to the greater excitability of inhibitory interneurons relative to excitatory pyramidal cells [53]. The recurrent terms $W_{nm}\cdot f\left[V_n\right]$ represent

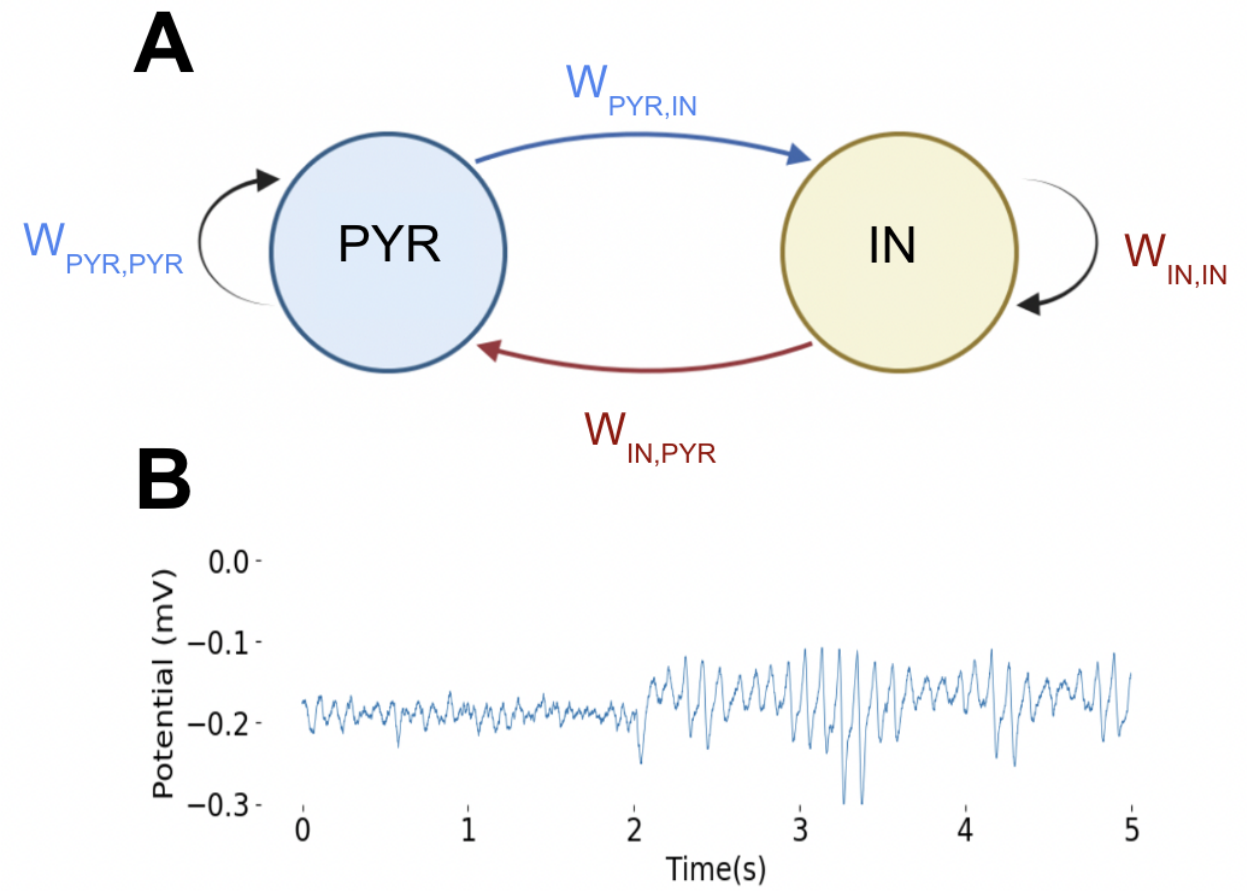

Figure 2: **Visual representation of Wilson-Cowan network with recurrent and reciprocal connections between pyramidal (PYR) and inhibitory (IN) neuron populations, along with an associated computationally generated seizure event**

(A) The parameter W_{PYRPYR} represents synaptic weights between excitatory populations, while the parameters W_{PYRIN} and W_{INPYR} represent synaptic weights between excitatory and inhibitory neurons. Lastly, the parameter W_{ININ} quantifies synaptic weights between inhibitory interneurons. (B) Membrane potential (mV) of a pyramidal population modeled using Wilson-Cowan equations illustrating normal transient activity between 0 and 2 seconds, and a seizure event between 2 and 5 seconds (Seizure is provoked by stimulation beginning at 2 seconds). Parameters used for this figure are summarized in Table 1. The code used to generate the figure can be found in Code 1

the effective synaptic input originating from one population. Together, these terms are proportional to the firing rate of that population, defined by f, by combining the proportion of the population that is firing, with the implications of this firing using the synaptic weight relevant to the connection ($n = PYR, IN$ — $m = PYR, IN$). The synaptic weights along with rate constant parameters are derived based on previous studies in our group, which used firing curves and weighting variables to yield seizure-like oscillatory dynamics [3]. Lastly, the additive terms $\sqrt{2D}\xi_{PYR,IN}(t)$ represent noise added to both excitatory and inhibitory neurons to mimic inputs from other brain areas that are not modelled explicitly. Specifically, D acts as a baseline noise amplitude parameter within the system, representing inherent noise from sources such as channel noise, thermal fluctuations and a variety of others [54]. Furthermore, since our system sits on the edge of a bifurcation point towards a seizure state, time-varying fluctuations can push the system past the seizure threshold thus acting as the seizure onset mechanism, similar to what one would expect from external stimuli (e.g. sensory stimuli). This can result in the seizure activity seen in Figure 1B, while further details about fluctuations over time can be seen in the code [55]. The term $\xi_{PYR,IN}(t)$ corresponds to independent Gaussian white noise processes of zero mean and unit variance, which simulates the stochastic nature of neural activity, and induces variability into the system [56].

In order to calculate the proportion of a neural population that is firing at any given time we use a Frequency-Input (F-I) curve, which outlines the relationship between neuronal input and likelihood of neuronal firing. This curve takes the form of a sigmoid function as determined by motor neuron population discharge experiments among others throughout the 20th century [57]. The idea is that most neurons lie dormant just below their threshold of activation, and when a neural population receives input, the number of neurons firing will increase exponentially with that input until a point where it levels off due to there being a finite number within the population. This schema lends itself to that of a sigmoidal curve defined by:

$$f\left[V_n\right] = \frac{1}{1 + e^{-\beta(V_n)}} \tag{3}$$

Where V_n represents the membrane potential, and n represents the population from which it hails ($n = PYR, IN$ for excitatory and inhibitory populations respectively). β is a unitless and variable constant that allows nonlinear gain to be fit to experimental data [3]. This function links membrane potential with firing probability of neuron populations, and thus defines its excitability. In order to scale this excitability, one can change the non-linear gain of activation β, or modulate the membrane potential V_n using methods to be discussed later on.

Using this model, one can generate dynamics that closely resemble those seen in focal seizures. To generate such seizure-like events (i.e. seizure onset), we use a numerical integration performed by the Euler-Maruyama method with time step dt (see Table 1) and using custom Python programs developed for that purpose. These codes have been made fully available, and can be found in Code 1.

1.6 Quantifying Neural Activity

Once computational tools such as Wilson-Cowan models have been used to generate recordings of neural activity, we must analyze the data in order to draw conclusions. While the eye test can give some insight in certain cases, standardized and quantifiable investigations are important to gain a greater and more holistic understanding.

Spectral Characteristics

Certain spectral characteristics are important to take into consideration. These characteristics can not only tell us about the relative severity, but also allow for direct comparison of computational models with biological data, thus validating both methods in the process. Two of the recurring properties we will be seeing are the spectral power, as well as the peak frequencies. The power allows for an understanding of relative severity of individual seizure events, where greater amplitudes of oscillation correspond to greater severity, as well as a characterization of pathological features in EEG data [58] [59]. Measuring the frequency

bands at which seizures oscillate also acts as a strong descriptor of pathological activity from an EEG perspective, as well as the method of comparison across our models and biological data. Frequency data can also be drawn from interictal activity, giving clues as to the mechanisms surrounding seizure onset [23]. In order to measure the power spectrum we must use a mathematical tool called a Fourier Transform. This tool identifies the resonating frequencies within an oscillating system, and characterizes their prevalence within the system through power spectral density. It has also become a foundational way for epilepsy researchers to understand EEG data due to the plethora of information it can provide [60]. The general form of a Fourier Transform is as follows:

$$\mathcal{F}(\omega) = \int_{-\infty}^{\infty} f(t) e^{-i2\omega\pi t}\, dt \tag{4}$$

where the time-domain function, $f(t)$, is transformed into its frequency-domain representation, $F(\omega)$. This is done by integrating the function over an infinite interval making it periodic, thus allowing us to take a Fourier Series of the function which gives us its resonant frequencies [61]. Importantly, when using the Fourier Transform, our results (Figure 3A) are plotted along a power spectrum as seen in Figure 3B. Peak spectral powers indicate the frequency at which the system is naturally resonating, and ensuing peaks are just harmonics of the oscillating system. In order to get power spectral density, PSD, we take the squared magnitude of the Fourier Transform as shown in the following equation:

$$PSD = |\mathcal{F}(w)|^2 \tag{5}$$

where $\mathcal{F}(w)$ denotes the Fourier Transform [62]. Overall there are a number of ways we will quantify our results, and using these differing methods we will be able to make inferences and draw conclusions about the data. Whether it is a direct conclusion surrounding severity of seizures, or a contrast between computational and biological data sets; these signal processing techniques applied to EEG data provide a method by which to objectively and numerically

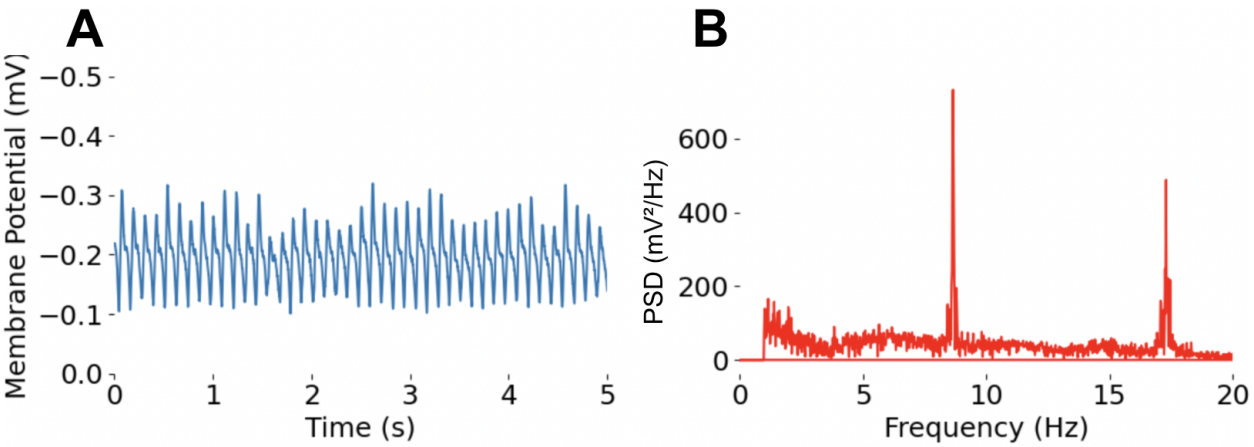

Figure 3: **Exemplar model seizure plotted next to its associated power spectrum** (A) Seizure event oscillating approximately 8-9 times per second, and created using the Wilson-Cowan model. (B) Fourier Transform derived power spectrum of the seizure event in panel A illustrating the power spectral density of the neural activity. Parameters used for this figure are summarized in Table 2. The code used to generate the figure can be found in Code 2

describe neural dynamics in pathological recordings.

1.7 Excitability heterogeneity and seizure predisposition

The implication of biophysical heterogeneity of neurons in seizure-like dynamics has notably been investigated using the Wilson-Cowan formalism [3] [63]. This was achieved by altering the excitability parameters of the populations, providing an understanding of how excitatory and inhibitory cell type heterogeneity affects seizure severity. It has been previously shown that a lack of diversity between neurons can predispose brain circuits to seizures. Diversity can manifest in many ways, including through morphology of cells, distribution of cell types, as well as overall excitability of populations [64] [65] [66]. When there is a lack of neural heterogeneity, neural firing becomes increasingly correlated, inciting a hypersynchronous state within the brain [3]. The firing of neurons within a population will become more correlated, and a specific input that may only recruit a fraction of a heterogeneous population is able to recruit a large portion of its homogeneous counterpart. Heterogeneity in neural systems has

notably been shown to act as a stabilizing mechanism, fostering non-epileptic activity [3]. Mass recruitment, resulting from a lack of heterogeneity, may lead to synchronous dynamics, and due to the underlying pathology it can become an epileptic seizure. By looking at the average firing probability versus the input current of homogeneous and heterogeneous neuron populations, we can visualize this phenomena and gain a more intuitive sense of what is going on. This investigation was a reproduction of previous results as well as a way to familiarize myself with Wilson-Cowan modelling formalism [3]. In order to do this we must modify the firing rate function (sigmoid) seen in Equation (3):

$$f\left[V_n, h_n\right] = \frac{1}{1 + e^{-\beta(V_n - h_n)}} \tag{6}$$

In this equation we have added in the rheobase h_n (where n = PYR or IN for excitatory or inhibitory populations respectively), which defines the inflection point of the sigmoid curve, and partially decides the excitability of a neuron relative to the input it receives [3]. By creating gaussian distributions of rheobase values, we can alter the standard deviation $\sigma_{PYR,IN}$, thus modifying the heterogeneity of excitatory and inhibitory cells independently. Through this characterization, the effect of various types of heterogeneity on cellular excitability are encapsulated, whether they be morphological, cell type distributions, biophysical variability, or others [3].

Mathematically, we add the rheobase in Eq. (3) as, $f \rightarrow f\left[V + h_n\right]$ and now have a distribution of excitability curves that are integrated according to the following equation:

$$F[V] = \int_{-\infty}^{+\infty} f(V + h)\rho(h)dh \tag{7}$$

thus giving a mean firing rate $F[V]$ of the population according to a distribution of neurons with differential excitability (i.e., $\rho(h)$), which replicates in vivo neuronal excitability experiments [3]. Our distribution has a mean and variance defined by, $\rho(h) \rightarrow N\left(0, \sigma_h^2\right)$ where $\sigma_{PYR,IN}^2$ takes on values between 2.5mV and 16.5mV, emulating in vivo experiments out-

lined in the research we try to reproduce by Rich et al, regarding the amount of stimulation required to incite activation of a neural population [3].

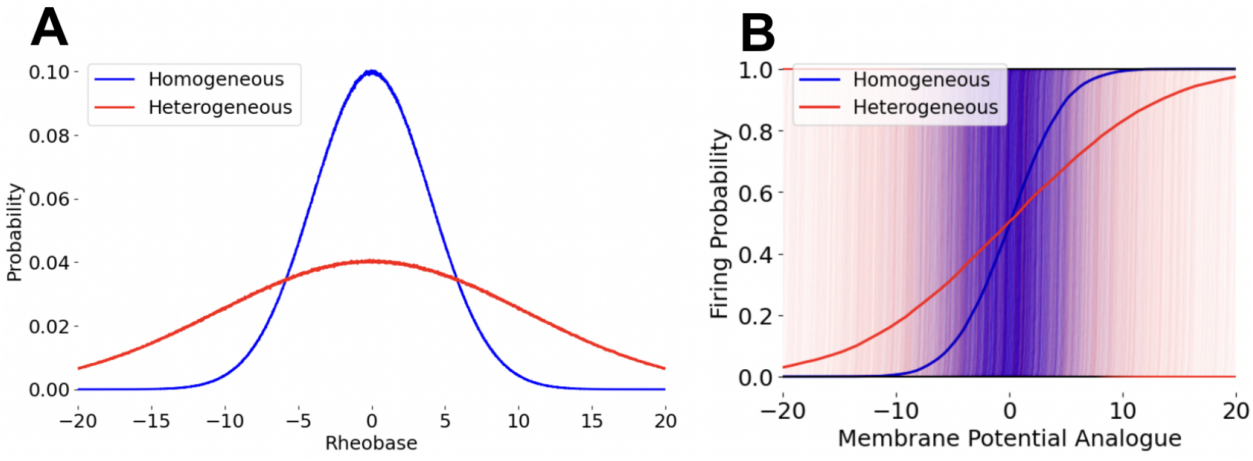

Figure 4: **Probability of neuron firing at different membrane potentials with heterogeneous and homogeneous neuron populations**

(A) Proportion of population becoming active relative to rheobase values, illustrating the distribution of homogeneous and heterogeneous populations according to a gaussian curve. (B) Firing probability of a heterogeneous neural population with a broad distribution of excitability thresholds, yielding a smooth mean firing curve (red). Firing probability of a homogeneous neural population with a narrow distribution of excitability thresholds, yielding a steep mean firing curve (blue). Firing probability of individual neurons within the excitatory and inhibitory populations that make up the mean firing curves. (Illustrated in light blue and light red. Parameters used for this figure are summarized in Table 1. The code used to generate the figure can be found in Code 1)

While viewing the F-I curves (Figure 4B) of homogeneous and heterogeneous populations, the rapid versus slow recruitment schema becomes easily visible. A steep curve appears in the homogeneous network, where small changes in membrane potential yield drastic changes in firing probability. This is further described by the probability distributions (Figure 4A) which shows the rheobase and firing onset probability of each population, where homogeneous networks are clearly more stark in their rapid recruitment. In contrast, the heterogeneous network has a much more linear curve (Figure 4B), where the same change in membrane

potential yields a smoother increase in firing probability, and thus less recruitment. Overall, this indicates homogeneous neural networks to have a greater propensity for seizure activity, as it requires far less input in order to cause mass activation within the network.

Building on the previous work summarized above to characterize neural heterogeneity, we used spectral analysis as a method to quantify seizure burden in the model [3]. The model is a Wilson-Cowan network with excitability heterogeneity incorporated, allowing quantification of spectral characteristics at differing values of $\sigma_{PYR,IN}$. These characteristics include power spectral density, peak spectral power, and the frequency of oscillation associated with peak spectral power, as shown in Figure 5. Neurons within a population can be deferentially excitable at a given membrane potential. For a population with low heterogeneity, most neurons will be deferentially excitable in a small range of membrane potentials, whereas populations with high heterogeneity would be the opposite, meaning there is a range of potentials over which the gradient in firing is seen. This means that we are likely to see larger fluctuations and greater degrees of hypersynchrony at lower heterogeneity measures. A greater amplitude of oscillation is in fact seen in both excitatory and inhibitory neuron populations in Figure 5, where decreased excitatory and inhibitory heterogeneity show the greatest magnitudes. Amplitude of oscillations can be used as a proxy for seizure severity, as larger oscillations are due to greater synchrony between neural populations. Furthermore, the lack of oscillatory activity seen in the upper right area of each heat map in Figure 5 reveals a strong protective effect induced by high levels of inhibitory heterogeneity. Our heat maps are corroborated by the computational EEGs in Figure 5A/B which match values of both frequency and amplitude measured in the heat map. One interesting trend that is observed (Figure 5C) runs counter to what one may expect. While the frequency of oscillation increases with lower inhibitory heterogeneity, the frequency actually decreases with reduced excitatory heterogeneity. This is an interesting finding as greater diversity within populations was expected to act as a protective effect against seizure burden regardless of neuron subtype. The use of frequency, as opposed to power, of oscillations, however,

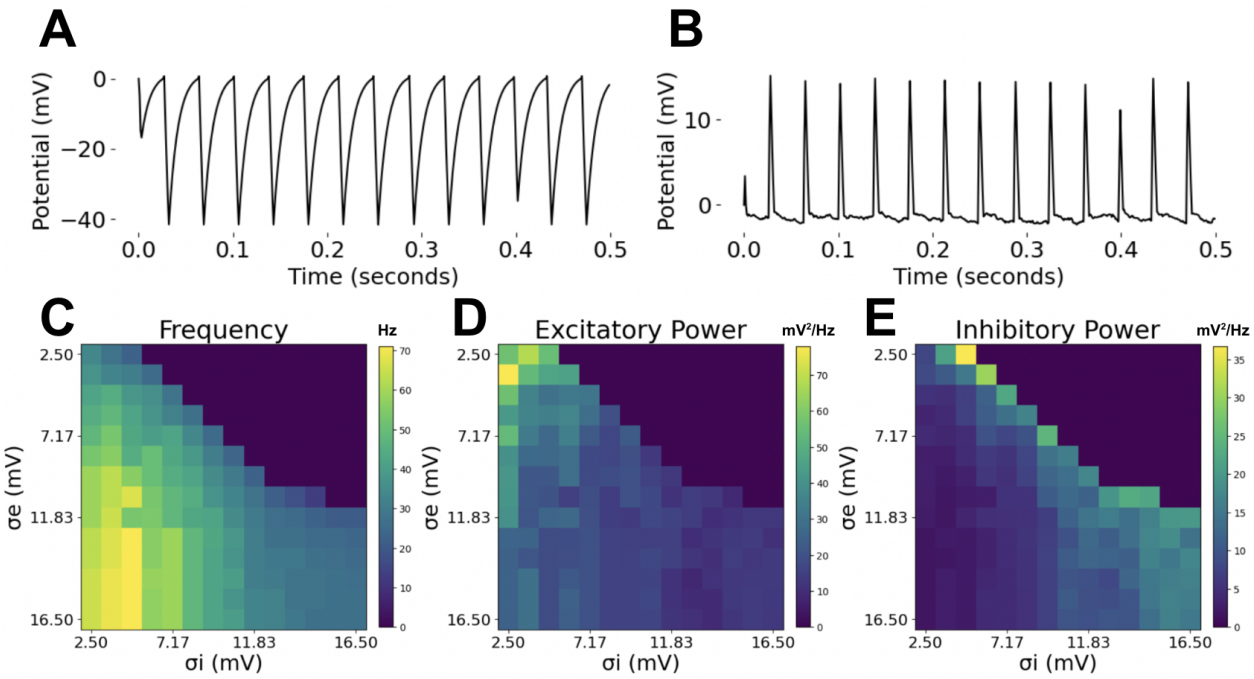

Figure 5: **Spectral properties of oscillatory EEG data relative to heterogeneity measures σ_{PYR} and σ_{IN}**

(A) Membrane activity of the excitatory and (B) inhibitory populations ($\sigma_{PYR} = 16.5$mV, $\sigma_{IN} = 12.5$mV). (C) Frequency of oscillations within the system, where peak frequencies arise at high levels of excitatory heterogeneity and low levels of inhibitory heterogeneity. (D) Peak spectral power of oscillations in the excitatory neuron population, where peak values appear at low levels of excitatory and inhibitory heterogeneity. (E) Peak spectral power of oscillations in the inhibitory neuron population, where peak values appear at low levels of excitatory and inhibitory heterogeneity, but also seem to rise with inhibitory heterogeneity. Parameters used for this figure are summarized in Table 1. The code used to generate the figure can be found in Code 1

as an indicator of epilepsy severity isn't necessarily the best metric, as there are many pathologies with differing oscillatory profiles which can vary greatly in terms of disease severity [67]. Furthermore, the frequency of oscillations can be variable during any given seizure, making it important to use other observations in conjunction with frequency when drawing insights about the data [17]. Overall, our investigation agreed with previous results showing that neural heterogeneity mimics many other types of diversity in nature, in that its presence acts as a stabilizing factor, whereas its absence is detrimental [3]. Furthermore, these investigations establish a solid foundation which can be used to understand how other parameters such as conduction delays, or myelinatory state influence oscillatory behaviour.

1.8 Discussion

Throughout this chapter we looked at modeling seizure activity with computational methods. We first introduced the prevalence and impact of epilepsy, emphasizing recent advances that suggest myelination plays a crucial role in neural network functionality and potentially in epilepsy. We then explored how ADM could influence seizure activity, suggesting a new therapeutic target. Next, we detailed the fundamental characteristics of neurons, focusing on the roles of excitatory and inhibitory neurons, providing a foundation for understanding the balance between excitation and inhibition, which is crucial in epilepsy research. We then delved into the disease itself, outlining its various types, pathologies, and the significant impact on those afflicted, emphasizing the difference between focal and generalized seizures along with the importance of understanding these differences for treatment and diagnosis. We then introduced seizure dynamics, in terms of the electrical activity in the brain picked up by EEG recordings, which can then be used to diagnose and understand epilepsy further. The following section saw an exploration of myelin as a pathology for epilepsy progression, discussing how specific patterns of myelination could influence neural activity and seizure dynamics. The Wilson-Cowan model was then introduced as a computational method for understanding epilepsy and neural dynamics. We outlined how the model can be modified

to investigate different parameters such as heterogeneity, as well as provided a mathematical representation along with ways by which we would quantify neural activity using spectral analysis. Lastly, heterogeneity was investigated for its role in seizure predisposition. We showed that a lack of neural heterogeneity could lead to increased seizure dynamics due to an increase in neural synchrony, confirming previous findings surrounding the topic [3].

Moving forward, a compelling extension of our current model is the incorporation of conduction delays, which arise due to a finite speed of action potentials along axons and across synapses. These delays significantly impact neural behavior by influencing the timing and synchronization of firing patterns. Including delays in the Wilson-Cowan model allows for a more biologically relevant representation of neural dynamics and helps us understand the role of timing in seizure propagation. Since myelination increases transmission speed, studying delays could reveal how changes in myelination impact seizure activity. Additionally, modeling these delays could uncover new therapeutic strategies which could target conduction delays in order to reduce seizure occurrences. By integrating these delays, we aim to create a more robust model that will better inform future research and therapeutic approaches.

It is important to note that the results presented in this section are a reproduction of previous experiments conducted by Rich et al., and that our results act to confirm observations in their study [3].

Chapter 2

Influence of Conduction Delays in E-I Networks

2.1 Chapter Summary

In this chapter, we begin with our motivation for incorporating conduction delays, to model the effect of myelin, within the Wilson-Cowan formalism established in the previous chapter. We then follow with a description of the methods used in order to construct our revised model. Next, we delve into the applications and results relating to underlying mechanisms for the dynamics seen in seizures as they relate to myelination and conduction delays. Finally, we conclude with a brief discussion of our methods and results, as well as their potential relevance to future investigations.

2.2 Motivation

As previously mentioned in Chapter 1, myelination has shown strong potential for being a pathological factor in progressive forms of epilepsy. ADM specifically, is known to cause seizure progression in mouse models [2]. Human forms of the disease have been treated with pharmaceuticals that impair disease progression with some efficacy, despite the previous lack of understanding surrounding the mechanism [2]. The greater disease burden is likely due to the increase in coherence between cortical areas at states of higher myelination, resulting in the hypersynchronous activity defining a seizure. Many brain functions depend on ADM. For example, memory impaired mice have shown significant improvement when myelination is promoted within the hippocampus, which is heavily implicated in memory and learning, thus illustrating the interplay between myelination, coherence, and cognitive function [43].

Overall, these findings underscore the importance of timing in neural processes, more specifically in epilepsy progression. According to research presented by Knowles et al., hyperactivity from seizures induces aberrant myelination, which then in turn causes more seizures. The delay between bilateral somatosensory cortical regions has been shown to decrease over time as myelin is added to relevant tracts, and as a result seizure dynamics increasingly proliferate throughout the brain. In order to better our understanding of the mechanisms at play, it is important to characterize the neural dynamics at differing stages

of disease progression. One way by which this can be accomplished is through analyzing different seizure characteristics according to conduction delays. To emulate differing states of myelination, we alter CV, and look at markers of disease burden such as seizure frequency, as well as mean and variance of firing rate within the populations. Changing CV gives a cross sectional view of the disease at different stages of progression, as disease progression is linked to increased myelination which is given by proxy with CV, while simultaneously elucidating an underlying mechanism of epilepsy progression as it relates to ADM. Furthermore, a cross-section style approach is particularly appropriate when considering the comparative time scales of neural activity and ADM. Where ADM takes considerably longer, anywhere from days to months, making a model that changes conduction velocity CV with respect to neural activity less applicable since it is relatively stable and can be considered constant at the scale of changes in neural dynamics [2]. Overall, this investigation introduces conduction delays in the Wilson-Cowan formalism, paving the way for a more holistic model that will emulate absence seizures in bihemispheric thalamocortical networks (Chapter 3).

2.3 Including conduction delays in the Wilson-Cowan model

In order to investigate seizure dynamics as it relates to conduction delays, we will be using the Wilson-Cowan models previously established and outlined in Equations 1 and 2, and inspiration from the way we characterized heterogeneity in the previous chapter. These equations describe mean membrane activity of interconnected excitatory and inhibitory populations in focal networks, which is modulated by the weighted firing inputs provided by each population. While this network is fairly simple, in that it doesn't provide a detailed description of specific neural tracts, it is actually very useful in understanding the basic mechanisms that underlie CV dependent seizure dynamics. Prior studies incorporating conduction delays into the WC models have demonstrated a significant connection between these delays and bifurcation phenomena, revealing that the timing of conduction delays can critically influence the system's stability and the transition between different dynamic states [68] [69]. The model

presented in Chapter 1, however, does not take into consideration conduction delays, and thus we must modify the equations to do so. Here, the dynamics of the the mean membrane potentials of excitatory pyramidal (PYR), inhibitory interneuronal (IN) obey::

$$\alpha_{PYR}^{-1}\frac{dV_{PYR}}{dt} = -V_{PYR} + W_{PYRPYR}\cdot f\left[V_{PYR}\right] + W_{INPYR}\cdot F\left[V_{IN}\right] + \sqrt{2D}\xi_{PYR}(t) \tag{8}$$

$$\alpha_{IN}^{-1}\frac{dV_{IN}}{dt} = -V_{IN} + W_{ININ}\cdot f\left[V_{IN}\right] + W_{PYRIN}\cdot F\left[V_{PYR}\right] + \sqrt{2D}\xi_{IN}(t) \tag{9}$$

where f has been replaced by F, which here indicates the mean activity taken over a distribution of conduction delays. To add conduction delays into the system, the weighted postsynaptic input in Equation 10 is averaged over a distribution $\rho(l)$ of axonal lengths, where inputs are assumed to propagate through axonal fiber tracts in which axons have variable lengths as follows,

$$F\left[V_{PYR,IN}\right] = \int_0^{+\infty} f\left[V_{PYR,IN}(t - \frac{l}{CV})\right]\rho(l)dl \tag{10}$$

where time delays are given by $\tau = \frac{l}{CV}$, with l being the lengths, and CV being the CV of axonal tracts amongst and between excitatory and inhibitory populations. Each individual axonal path gives rise to a given firing input to the postsynaptic population, and by adding all of these together, an average input value can be calculated through the term $F[V_{PYR,IN}]$. This firing rate term naturally takes into account synchronization, since signals coordinated in time will likely result in a compounding effect, as they are more likely to have similar potentials. As previously mentioned, in order to include myelination in the model, CV is used as a proxy, since myelination is directly related to the speed at which signals are transmitted along axons. It is important to note that recurrent connections, where a population self-synapses, will not have delays as we have assumed that there is negligible distance between a population and itself. Overall, this revised phenomenological model is able to take into

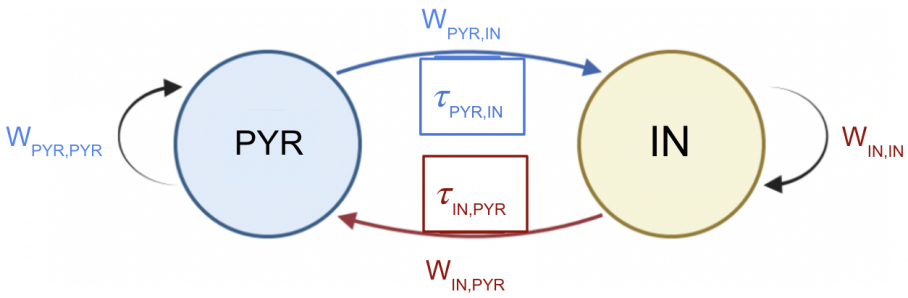

Figure 6: **Visual representation of Wilson-Cowan network with recurrent and reciprocal connections between excitatory pyramidal and inhibitory interneuron populations with conduction delay incorporated into the model.**

The parameter W_{PYRPYR} represents synaptic weights between excitatory populations, while the parameters W_{PYRIN} and W_{INPYR} represent synaptic weights between excitatory and inhibitory neurons. The parameter W_{ININ} quantifies synaptic weights between inhibitory interneurons. Parameters τ_{PYR-IN} and τ_{IN-PYR} represent the conduction delay from the excitatory to inhibitory, and inhibitory to excitatory populations respectively. Parameters used for this figure are summarized in Table 1. The code used to generate the figure can be found in Code 1

account biologically derived data surrounding conduction delays, such as CV and axonal tract lengths, allowing for investigation of neural dynamics at differing lengths of axons and speeds of neural transmission.

Using this model, one can generate dynamics that closely resemble those seen in focal seizures, that take CV into account. To generate such seizure-like events (i.e. seizure onset), we have noise amplitude fluctuations push the system past a bifurcation point and towards a seizure event.

Seizure Rate

One of our primary goals is to gain an understanding of seizure burden from the computational data, and thus indicators that can be drawn from EEG data are of central focus. One of the more obvious indicators is seizure rate, which can connect experimental with clinically measured data, as well as provide a strong correlate for quality of life [70] [71]. While it is fairly easy for the trained eye to spot a seizure on an EEG, once longer and a greater number of computational simulations are underway, it becomes an impractical approach. This problem necessitates a computational way of detecting and counting seizures. While there are many different algorithms used to detect seizures, there is no one size fits all method, furthermore non pathological oscillations occur that should not be classified as seizure events, and thus discretion must be used depending on the seizure type [72].

The method we will employ is done by counting and clustering oscillatory peaks seen during a seizure event, allowing for delineation between events. When a seizure occurs, fluctuations in membrane potential increase drastically and oscillate in a certain frequency range, allowing peaks (or maxima of an oscillation) to be counted based on a threshold value for membrane potential. Peaks that are close together are put into a single cluster and counted as one seizure event. In order to ensure non pathological peaks are not counted we apply a Butterworth filter to EEG data in order to isolate the desired frequency range (1Hz - 40Hz) unique to the seizures at hand. The Butterworth filter removes data outside of desired

frequency ranges thus allowing isolation of seizure activity in a data set [73]. Once this has been accomplished, we must separate seizure events to ascertain a proper count and thus frequency. To do so, we can cluster large peaks together if they occur within a certain time period. Since the oscillations are typically bordering the theta and alpha frequency bands between 6-10Hz, giving a grace period of 300ms, prior to delineation of a new event, allows for the slower seizures to be properly recognized without including distinct seizure events together when there another seizure event shortly thereafter [2] [23]. This approach can be modulated to fit with different periodic oscillations, and is thus ideal for our EEG data with its consistent frequencies.

2.4 Results

Exemplar Seizures

Using our new model, mean activity within populations is now influenced by conduction delays, creating focal seizure events with qualitative features close to real seizure events. These new qualities are illustrated in Figure 7, and give a visual representation of the recordings from which we will yield our results. The HYP seizure illustrated in Figure 7 exhibits characteristics similar to those observed in vivo, as in Figure 1, particularly notable are the fast oscillations during the ictal onset, which correspond to the tonic phase,. As the seizure progresses towards termination, there is a gradual reduction in frequency, transitioning into the clonic phase, where the frequency and intensity of muscle contractions begin to decrease [74]. Seizure events were triggered with noise causing a shift past the bifurcation point towards a seizure. It also notably mimics appropriate ranges of membrane potential during the ictal period, lending further support to the use Wilson-Cowan models in our investigation.

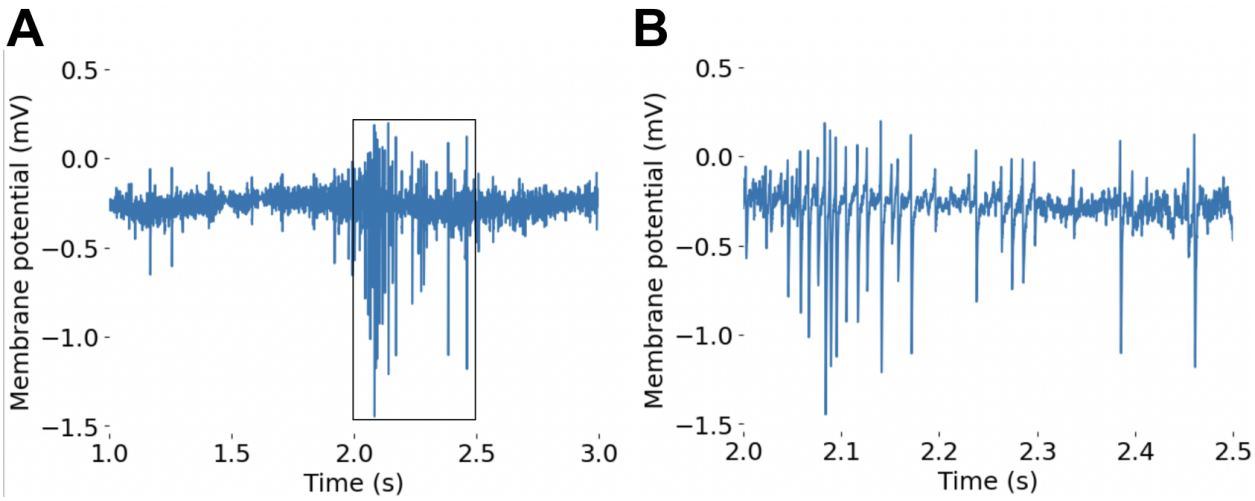

Figure 7: **Simulated mean membrane activity of a focal seizure event incorporating delays which emulate myelination**

(A) Membrane activity of the excitatory population of a Wilson-Cowan model with a CV of 1m/s, recorded from 1-3 seconds (B) Mean membrane activity of population described in (A) illustrating recordings from 2-2.5 seconds to illustrate a close-up seizure event. Seizures were triggered through gaussian white noise in the system. Parameters used for this figure are summarized in Table 1. The code used to generate the figure can be found in Code 1

Seizure Burden

Characterizations of neural activity in relation to epilepsy can take many different forms. One important measure is that of disease burden. Disease burden can tell us the relative progression of the disease as it relates to different parameters, one being CV. Furthermore, it can be quite difficult to align computational models with clinical data, and seizure burden offers a way by which to accomplish this goal. With CV being used as a proxy for myelination, we are trying to understand how myelination affects overall disease progression. In order to assess the relative burden of epilepsy from a computational perspective, seizure rate can be taken into account as a proxy for overall disease severity. While looking at seizure rate, it is important to note that the Wilson-Cowan model is phenomenological in nature, meaning that parameters can be adjusted to biologically relevant values in order to potentially view specific numerical trends that would be seen in vivo. However, the general trend of the data will remain constant regardless of the specific numerical values one may choose, unless plasticity is explicitly modeled, which is not the case here [2]. In this case, CV has been chosen according to published data regarding speed of neural impulses along axons (0.05m/s - 1m/s), as well as consideration for proper visualization [75].

As seen in Figure 8A, there is a clear observable trend where increases in CV are associated with an increase in number of seizure events per hour. This trend runs in line with our hypothesis, and supports previous results found in mouse models linking hypermyelination to epilepsy progression [2]. The specific shape taken by the data is also of note, where it approaches a saturation as CV increases. When considering the characteristics of the model, it makes sense that there is an upper limit to seizure rate since delays can only get so small, meaning there is a point of diminishing returns as CV is increased. This idea runs in parallel to myelination of neural tracts, where they can only be myelinated to a certain degree as there is a finite length of axon to be myelinated, at which point CV will reach a saturation, thus resulting in a minimum delay. This is further supported by Figure 8B, which shows peak spectral power to increase with CV, also showing signs of saturation. Being another

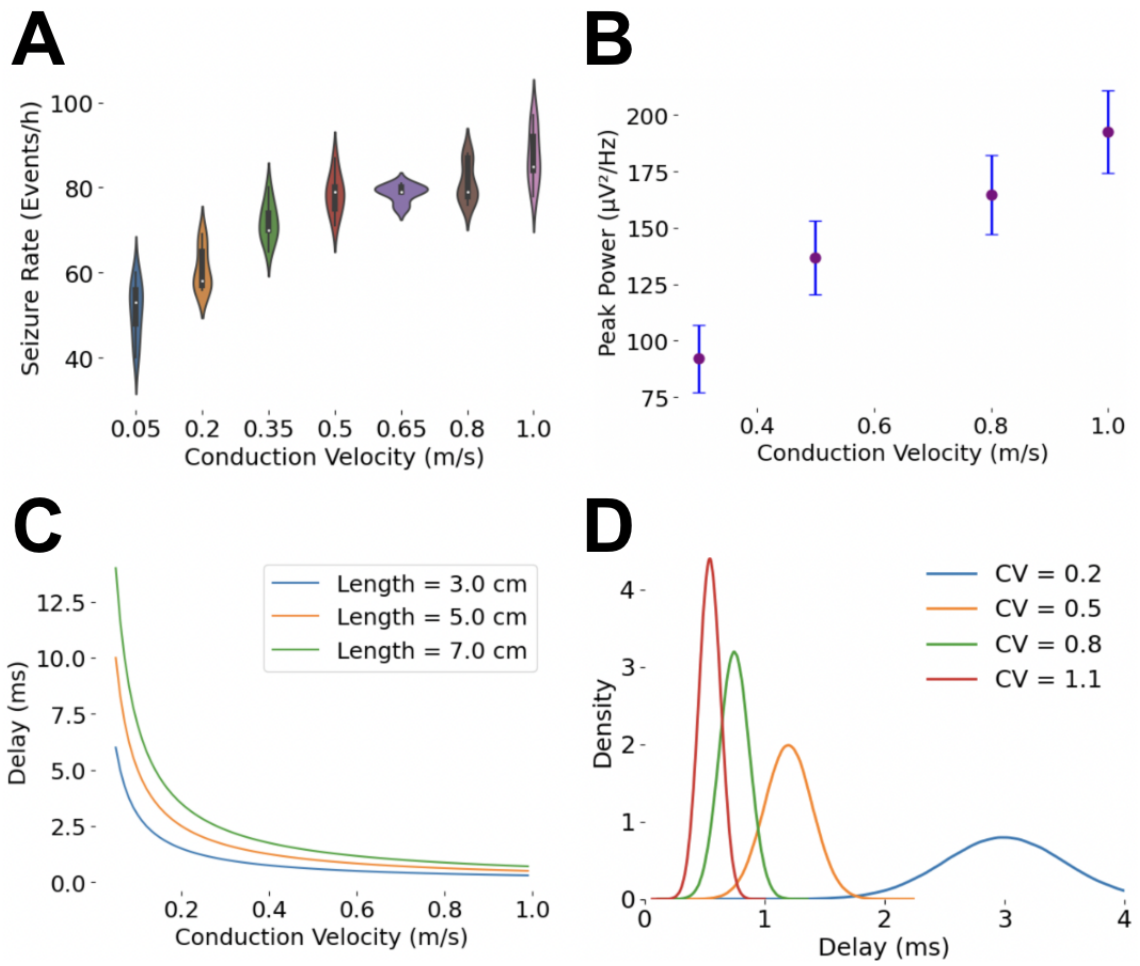

Figure 8: **Seizure burden and conduction delay relative to CV**

(A) Seizure rate is measured in seizures events per hour. CV ranges from 0.05m/s-1m/s, acting as a proxy for myelination state in the Wilson-Cowan model. Error bars indicate variability over trials. (B) Peak spectral power spectral density of oscillations relative to CV, illustrating a positive trend where higher CVs are associated with increased peak spectral powers. Simulation created over 10 trials, each trial spanning 20 seconds. (C) Delay is measured in milliseconds, and CV is measured in m/s. Axonal lengths are 3cm, 5cm, and 7cm. (D) Delays are measured in milliseconds, whereas density is unitless. CV of distributions is coded by colour, with high conduction velocities yielding distributions with the least variance. Parameters used for this figure are summarized in Table 1. The code used to generate the figure can be found in Code 1

measure of seizure burden, the increase of peak spectral power relative to CV indicates that increased myelination is indeed pushing the system towards more severe seizure dynamics, thus supporting our hypothesis. Additionally, the lower bound on conduction delays exists since the average length of the tracts does not change. This idea is better visualized in Figure 8C where delays are decreasing relative to CV, but doing so in a way that clearly levels off at higher levels of measures CV, thus reinforcing the reasoning behind seizure rate increasing in smaller increments at higher rates of CV as illustrated in 8A, as a saturation is reached.

Conduction Delay Hypothesis

While it has become apparent through previous research along with our computational investigations that high levels of myelination can promote hypersynchrony, the underlying mechanisms are still poorly understood [2]. We build on the approach used to study heterogeneity in Chapter 1, where increasing diversity reduces seizure burden. However, in the case of CV, instead of diversity in neuronal excitability, our hypothesis revolves around diversity of conduction delays. Our hypothesized mechanism is the following: **homogenization of conduction delays increases the likelihood of presynaptic inputs being correlated. Therefore, by homogenizing delays, through increase in CV, the synaptic input becomes far more correlated, allowing for large fluctuations of membrane potential within populations, which can induce hypersynchronous events, also known as a seizure.**

In Figure 8D it becomes much easier to understand the motivation for this hypothesis, where a high CV leads less variance in conduction delays. This idea is very important, as it could form the basis for myelination as a pathological factor in epilepsy. In order to fully visualize it, Figure 9 provides an illustration of highly heterogeneous versus non heterogeneous delays, as well as their potential resulting dynamics. It is important to note that Figure 9 indicates conduction delays an order of magnitude larger than those previously discussed, and

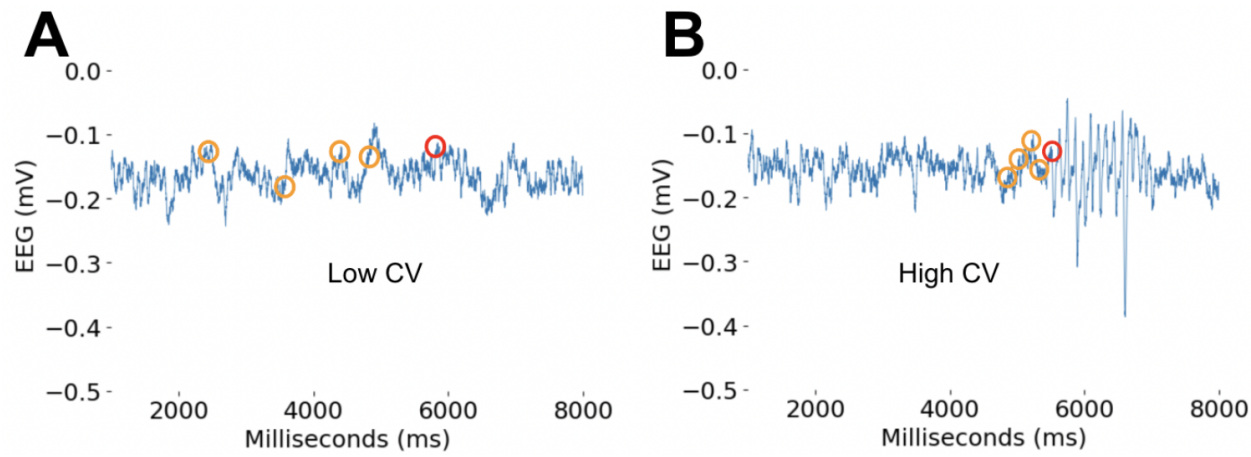

Figure 9: **Illustration of delay distribution at high versus low conduction velocities visualized on and EEG time series**

The orange circles indicate where inputs arise due to delays, and red circles indicate the point at which they are being integrated. (A) Case of low CV (0.2 m/s) where input potentials are heterogeneous in time. (B) Case of high CV (1.1 m/s) where input potentials are highly correlated in time. The delays used in this figure were chosen to help visualize the mechanism, and are not numerically meaningful. Parameters used for this figure are summarized in Table 1. The code used to generate the figure can be found in Code 1

are for illustrative purposes only used in our models. Instead they are meant to illustrate the difference between high and low correlation of inputs. In Figure 9A, the low CV of 0.2 m/s allows for less correlated input which acts as protection from seizure dynamics, whereas in Figure 9B, the higher CV of 1.1 m/s allows for correlated input yielding hypersynchronous seizure dynamics, illustrated just prior to the 6 second mark of the computational EEG recording. It is important to note that these simulations were not given external stimulation, instead CV is responsible for the differential dynamics. The key takeaway is as follows: faster signal transmission causes higher levels of correlation between inputs, thus opening the door for larger amplitude fluctuations.

Influence of CV on Firing Rate Mean and Variance

We are starting to understand how CV is affecting the simple Wilson-Cowan E-I network, but there are still important characterizations of the underlying mechanisms that need to be done. We are now trying to pinpoint the dynamical mechanism based on the observations made previously, which indicate myelination to be the driving factor, while also investigating potential confounding parameters. Furthermore, finding the aspect of neural activity influenced by CV inducing seizure-like activity is of quintessential importance. As it stands, variance is the primary suspect, where an increase in CV results in higher degrees of variance in pre-ictal EEG data, thus increasing propensity towards a seizure state. While this mechanism makes intuitive sense, a stronger characterization relative to CV is in order. Furthermore, noise should be included, as it allows for differentiation between pathological factors, and elucidates an understanding of the extent to which each factor contributing to the pathology. Another factor that could influence the susceptibility to seizures is mean membrane potential, where myelination or noise could push the membrane potential to values that allow for easier transitions to seizure states.

Mathematically, we can explore how changes in noise amplitude and CV influence the mean firing rate of our system by examining the following average,

$$F[\tilde{V}] = \int_0^\infty f[V(t-\tau)]\rho(\tau)d\tau \tag{11}$$

where the membrane potential $\tilde{V}$ has been replaced here by the following Ornstein Uhlenbeck process with noise variance $\sqrt{D}$,

$$\frac{d\tilde{V}}{dt} = -\tilde{V} + \sqrt{2D}\xi \tag{12}$$

In Equation 11, we see the mean firing rate $F[\tilde{V}]$ as a function of the membrane potential $\tilde{V}$ integrated over the delay parameter τ, which is weighted by a delay distribution function $\rho(\tau)$.

As described, the function $F[\tilde{V}]$ describes the cumulative effect of the membrane potential at a delayed time $t - \tau$ on the current firing rate. In Equation 12, we omit weighted firing seen in the Wilson-Cowan equations (i.e., Eq. 2) allowing the influence of variance and CV to be of sole importance. Taken together, this allows us to examine the effect of D and CV on the mean and variance of the firing rate $F[\tilde{V}]$. The results described in Figure 10, regarding

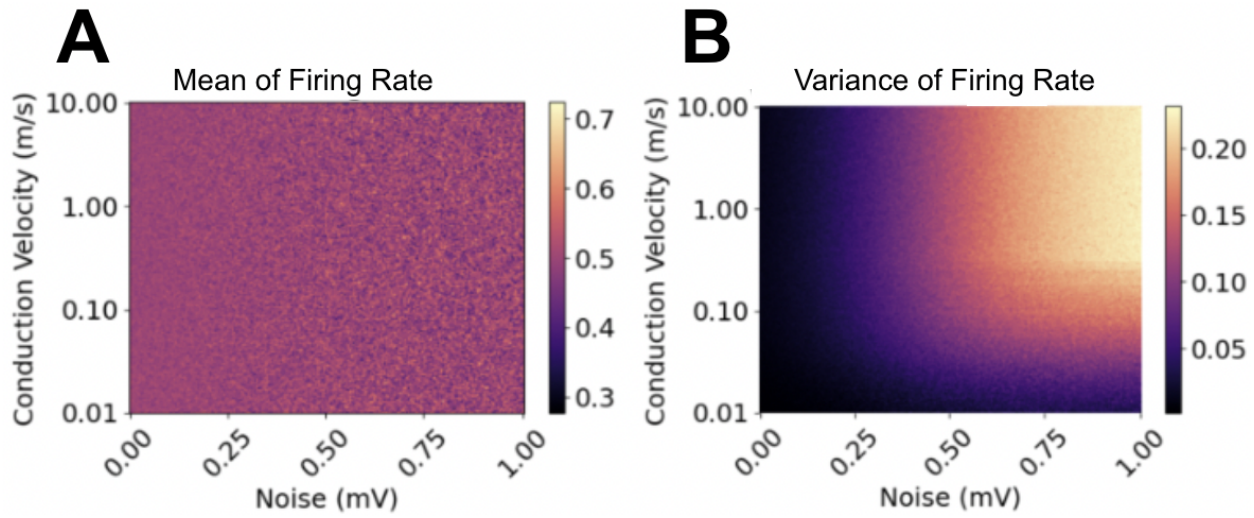

Figure 10: **Effects of noise and CV on variance and mean firing rates**

(A) Variance of firing probability ($F[\tilde{V}]$) with respect to CV and noise amplitude (B) Mean of firing probability ($F[\tilde{V}]$) with respect to CV and noise amplitude. CV values range from 0.01m/s-10m/s. Noise values range from 0mV-1mV. Parameters used for this figure are summarized in Table 1. The code used to generate the figure can be found in Code 1

firing rate mean and variance, support the idea of hypermyelination being pathological in epilepsy. As can be seen in Figure 10B, increases in noise cause higher variance in the firing response, as expected, and the CV does as well. This indicates that myelination takes the system towards a state of higher variance. The gradient is especially clear between 0.05m/s and 1m/s, where variance increases dramatically. Considering these are biologically relevant values, the stark contrast provides strong support for myelination as the underlying mechanism. Additionally, the mean firing rate stayed relatively stable, as can be seen in Fig 10A. This stability in mean firing rate indicates that there was no shift in average membrane

potential allowing for an easier path towards seizure activity, thus isolating CV as the key pathological factor. This result aligns with what is expected from delay differential equations: time delays do not change the fixed points of a system, but influence its predisposition to oscillatory behaviour and its response to noise or fluctuations [76].

2.5 Discussion

Taken together, these findings illustrate the relationship between myelination and seizure dynamics from a computational perspective. The idea that increased myelination promotes synchrony is supported in Figures 8A and B where a greater CV has a clear positive relationship with seizure rate as well as peak spectral power in the Wilson-Cowan model. As previously discussed, the data reaches a saturation, meaning that as the CV increases, seizure rate increases at an increasingly slower rate. This relation makes sense and can be intuited by thinking about myelination in the brain. Axons have a limit to the amount of myelin that can surround them, and when you come closer to reaching that limit, the increase in myelination has less of an effect, as the delay is already quite close to its minimal value. The computational model lives by the same rules, where input delays can only get so small as the CV is increased, and when it gets close to 1m/s, the delay and thus seizure rate approaches its maxima. A more mechanistic understanding of the increase in seizure rate can be described by input synchrony. If delays are large, then inputs are likely to be diverse, yielding protection from hypersynchrony. However, when delays are small, inputs into the neural populations are likely to be more synchronized in time, and thus their inputs are likely to be more similar. This means otherwise "normal" membrane fluctuations may yield seizure events, as input to the population becomes correlated, causing a compounding effect that can push a system into a state of hypersynchrony. This is shown in Figure 10B where increases in CV yield higher variance within the population, thus supporting our hypothesis stated earlier in Chapter 2. It is also important to note that Figure 10A shows no change in mean firing rate, which could be a confounding variable, meaning CV induced variance is

driving the system to seizure states.

The simple Wilson-Cowan system used in this chapter does however have some limitations. Firstly, being a phenomenological model that aims to reproduce macro activity within cortical columns, certain mechanisms underlying this activity may be difficult to elucidate. For example, mutations in voltage gated sodium ion channels in the reticular thalamic nucleus are known to induce epilepsy, however, specific investigations regarding this pathology are somewhat limited as ion channels are not present within the model [77]. Furthermore, the simple two population model used here does not bring about many specific understandings of neural circuits within the brain, such as implications in specific areas, or along certain tracts. Although it provides underlying mechanisms for general trends, a more complex system of Wilson-Cowan equations would be in order to properly contrast with biological data, as epileptogenic circuits tend to be more complex than just a singular excitatory and inhibitory interaction. Furthermore, this simplicity prevents investigations surrounding seizure generalization since there is only one inhibitory and excitatory population, meaning these results mostly pertain to focal seizures confined to a given area within the brain. Overall, these results illustrate an important mechanism for seizure progression, but also a need for a more complex model that allows for investigation of specific epileptogenic tracts, as well as propagation of seizure dynamics.

Chapter 3

Myelination and Absence Seizures in a Bihemispheric Thalamocortical Network

3.1 Chapter Summary

In this chapter, we begin by outlining the reasons for creating and using a bihemispheric model when contrasting our data with in vivo recordings from research partners, where the absence seizures observed in the bihemispheric thalamocortical networks necessitate a model spanning a greater spatial scale. We follow this up with a discussion of the specific computational methods used in order to define our new model. Next we show the applications of this model in a few distinct ways; first, we contrast computational and biological data sets; second, we use the model to provide guidance to future experimentation; third, we use the model as well as its underpinnings to explain the mechanisms for myelin related seizure progression. Lastly, we conclude with a discussion our work, as well as its implications on our understandings of epilepsy.

3.2 Motivation

While the previous investigation using a local two population Wilson-Cowan model gave some valuable insights, there are still important questions that require expansion of our model. One of the big questions we have yet to talk about relates to the generalization of seizures and whole brain networks. The local model (Chapter 2) creates an understanding of focal dynamics between two populations, however, in the brain there are a number of populations at play which must be accounted for. In seizure networks specifically, the oscillatory activity takes form of absence seizures in thalamocortical loops, elucidating the need for populations at the thalamic as well as cortical levels [78]. By creating a thalamocortical network, we can model absence seizure activity occurring in relevant biological models, instead of the focal HYP/LVF seizures modelled previously. The experimental research was done in the Scn8a mouse model, which develops epilepsy due to a sodium gated ion channel mutation in reticular thalamic populations (Scn8a+/mut) [79] [2]. However, if ADM of callosal tracts is prevented through oligodendrocyte precursor conditional knockout (Scn8a+/mut OPC cKO), one can see a stark reduction in seizure activity. This suggests that pathological

oscillations are able to generalize through the corpus callosum where they spread throughout the brain, highlighting the need for a bihemispheric model [80]. This framework will allow us to understand the interplay between inter-hemispheric populations, create contrasts with biological data, and guide future experimentation with the efficiency of computationally derived data. It also has substantial support from previous literature which outlines generalized absence seizures in thalamocortical circuits as the primary type of seizure in many different epilepsy types, specifically those relating to developmental childhood epilepsy's [37] [81]. The thalamocortical circuit discussed is comprised of two oscillating systems, which are connected by the corpus callosum, allowing them to influence each other. Their influence on each other is dependent on conduction delay timing between the two oscillating circuits, thus underlining the importance of callosal myelination in this pathology [82] [83]. Through differential myelination and a bihemispheric framework, we elucidate an absence seizure model that can investigate the effect of ADM using a cross sectional approach.

The prevalence of generalized absence seizures in developmental epilepsy's strongly favours the ADM pathology, as ADM provides a mechanism by which seizure burden can increase with time. The model also includes another crucial piece revolving around callosal myelination states. In previous studies, seizure associated callosal tracts have shown differential myelination, where increased seizure activity is associated with more myelin [2]. Incorporation of callosal myelination as a variable will thus provide an understanding of its role in seizure dynamics. One important thing to note is that the bihemispheric model was created in order to contrast our data with biologically derived data from the Knowles Lab at Stanford. Their experiments (many unpublished) have helped give biological constraints to our model, allowing direct comparison between Wilson-Cowan modelling and in vivo EEG results through calibration between the two. Overall, this collaboration allows us to verify the validity of the model, as well as use it to guide future experimentation and answer further questions surrounding myelination and epilepsy. These questions also bring about predictions, whereby we expect measures of seizure burden to increase along with CV of the

callosal tract. Specific measures will be explored further later on, but take similar forms as those seen in Chapter 2.

3.3 Methods

In order to create the bihemispheric model, we will mostly be using the same framework as before, however with some important modifications and expansions. One such modification is that we will no longer be using noise amplitude as the method for provoking seizures. Instead we will now apply direct stimulation to the thalamic populations, allowing for more control surrounding seizure onset. This method is preferable for our bihemispheric model as our primary goal is to compare and contrast spectral properties computational and biological data sets. Having the control over seizure onset allows for simpler quantification and comparison between recordings. Furthermore, we will be incorporating callosal myelination state, since communication, and thus activity between the two hemispheres is heavily dependent on the conduction delays present between excitatory cortical areas through the corpus callosum [2]. In order to do so we use callosal CV as well as tract length values recorded by our research partners (Knowles lab, Stanford) to inform our computational investigations. We must also address the increased number of neural populations (Visual representation provided in Figure 11. In our model we will create representations of an inhibitory reticular thalamic nuclei population, excitatory ventrobasal thalamic population, and both excitatory and inhibitory populations in the somatosensory cortex. The somatosensory cortex was chosen as our cortical area due to it being a hotbed for absence seizure activity, especially in the mice studied by our research partners [2]. The ventrobasal thalamic population is heavily implicated in projections to the somatosensory cortex, and is thus well suited to represent our excitatory thalamic population [84] [85]. On the other hand, the reticular thalamic nucleus is an inhibitory population known to modulate seizure activity, meaning its presence in our model is important to create a proper representation of a thalamocortical network [19]. The populations are differentiated by their polarity, with inhibitory populations being nega-

tive, as well as the weighted connections, membrane time constants, baseline noise, and the unique projections sent to each population.

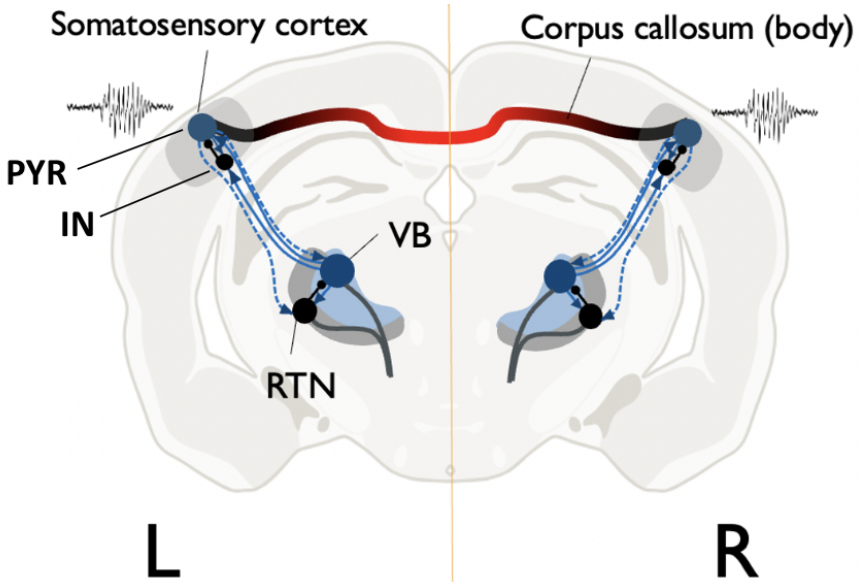

Figure 11: **Visual representation of the bihemispheric model**

Connections between excitatory (blue) and inhibitory (black) populations of the thalamocortical bihemispheric model are shown according to their effect (blue = excitatory, black = inhibitory). The ventrobasal thalamus (VB) and reticular thalamic nucleus (RTN) are labeled as the relevant thalamic populations. The pyramidal (PYR) and interneuron (IN) populations are labeled as the relevant cortical populations. Right and left hemispheres are denoted by "R" and "L" respectively. The somatosensory cortex is labeled as the relevant cortical area. The corpus callosum connects excitatory cortical areas, allowing for interhemispheric communication (Graphic created by Dr. Jeremie Lefebvre)

Figure 11 gives a visual representation of the bihemispheric model, where inhibitory populations synapse onto local excitatory populations, excitatory populations synapse onto each intrahemispheric population, and somatosensory cortical areas synapse onto each other using the interhemispheric connection provided by the corpus callosum. This schema is supported by our collaborators (Knowles lab, Stanford), where anterior portions of the corpus callosum connecting the somatosensory cortices together show differential myelination, implicating this specific tract in the pathology [86]. To incorporate this idea we must connect these areas in our mathematical model; this can be accomplished using Equation 10 where callosal tract lengths and conduction velocities inform the bilateral input between somatosensory areas.

Mathematically, the mean membrane potentials of excitatory pyramidal (PYR), inhibitory interneuronal (IN) of the somatosensory cortex, along with the ventrobasal, and reticular thalamic populations of the thalamus are influenced by a variety of intrahemispheric (I), and contra-hemispheric (C) synaptic inputs. These can be described with the following differential equations given in vector form:

$$\mathcal{D}\mathbf{V}^{r,l} = I[\mathbf{V}^{r,l}] + C[\mathbf{V}^{r,l}] + \mathbf{B}^{r,l} + \mathbf{S}^{r,l} + \mathbf{N}^{r,l} \tag{13}$$

where r and l refer to the right and left hemispheres, and $\mathbf{V}^{r,l} = \left[V^{r,l}_{\text{PYR}}, V^{r,l}_{\text{IN}}, V^{r,l}_{\text{VB}}, V^{r,l}_{\text{RTN}}\right]^{-1}$ represents the mean membrane potentials of the populations previously described and shown in the equation.

The differential operator defined by $[\mathcal{D}]_m = (1+\alpha_m \frac{d}{dt})$ incorporates unique time constants α_m for each population in the network. The index m can represent populations such as PYR, IN, VB, or RTN as shown in Eq. (13). The expression $[\mathbf{B}^{r,l}]_m = B^{r,l}_m$ denotes constant baseline currents for each population. Meanwhile, $[\mathbf{S}^{r,l}]_m$ represents external stimuli, which are initially set to $\mathbf{0}$. Lastly, the term $[\mathbf{N}^{r,l}]_m = \sqrt{2D_m}\xi^{r,l}_m$ takes into account independent random fluctuations characterized by Gaussian white noise $\xi^{r,l}_m$ with a mean of 0, and acting upon each population separately.

In Eq. (13), the synaptic inputs within either hemisphere are of three types: cortico-cortical (CC), intra-thalamic (IT), and cortico-thalamic (CT).

$$I[\mathbf{V}^{r,l}] = \underbrace{W_{\mathrm{CC}}\mathbf{F}[\mathbf{V}^{r,l}]}_{\text{cortico-cortical}} + \underbrace{W_{\mathrm{IT}}\mathbf{f}[\mathbf{V}^{r,l}]}_{\text{intra-thalamic}} + \underbrace{W_{\mathrm{CT}}\mathbf{f}[\mathbf{V}^{r,l}(t-\tau_{\mathrm{CT}})]}_{\text{cortico-thalamic}} \tag{14}$$

The response function $\left[\mathbf{F}[\mathbf{V}^{r,l}]\right]_m = F[V_m^{r,l}] = \frac{1}{1+e^{(-\beta V_m^{r,l})}}$ allows us to infer the overall firing rate of a neural population according to its mean membrane potential in the Wilson-Cowan model. In Eq. (14), a time delay τ_{CT} is added to incorporate the finite conduction time along thalamocortical pathways. Additionally, the synaptic weights that influence interactions within and between cortical and thalamic populations given by the following set of matrices:

$$W_{CC} = \begin{bmatrix} w_{\mathrm{PYR,PYR}} & w_{\mathrm{IN,PYR}} & 0 & 0 \\ w_{\mathrm{PYR,IN}} & w_{\mathrm{IN,IN}} & 0 & 0 \\ 0 & 0 & 0 & 0 \\ 0 & 0 & 0 & 0 \end{bmatrix} \tag{15}$$

$$W_{IT} = \begin{bmatrix} 0 & 0 & 0 & 0 \\ 0 & 0 & 0 & 0 \\ 0 & 0 & 0 & w_{\mathrm{RTN,\ VB}} \\ 0 & 0 & w_{\mathrm{VB,\ RTN}} & 0 \end{bmatrix} \tag{16}$$

$$W_{CT} = \begin{bmatrix} 0 & 0 & w_{\mathrm{VB,PYR}} & 0 \\ 0 & 0 & w_{\mathrm{VB,IN}} & 0 \\ w_{\mathrm{PYR,VB}} & 0 & 0 & 0 \\ w_{\mathrm{PYR,\ RTN}} & 0 & 0 & 0 \end{bmatrix} \tag{17}$$

We assume that synaptic inputs originating from the contralateral hemisphere occur exclusively between cortical pyramidal (PYR) populations located on opposite sides, meaning $\left[C[\mathbf{V}^{r,l}]\right]_m = 0$ whenever $m \neq \mathrm{PYR}$. Additionally, these inputs travel through callosal tracts

comprised of K axons, each with differing conduction velocities. As a result, the contribution from the opposing hemisphere in Eq. (13) can be given by the following equation:

$$\left[C[\mathbf{V}^{r,l}]\right]_{\mathrm{PYR}} = w_{\mathrm{callosal}} K^{-1} \sum_{k=1}^{K} F[V_{\mathrm{PYR}}^{l,r}(t - \tau_{\mathrm{callosal},k})] \tag{18}$$

where $\tau_{\mathrm{callosal},k} = \ell / c_k$ refers to the conduction delay between hemispheres along axons with a length of ℓ and a range of conduction velocities given by c_k (ranging from 0.5m/s - 1.5m/s). In order to trigger seizure events, stimulation can be applied to thalamic populations, which induces hypersynchrony in the theta band throughout the thalamocortical network.

Using the model defined above, we can now illustrate and verify the qualitative comparison between biological and computational data in Figure 12. Figure 12A depicts a compu-

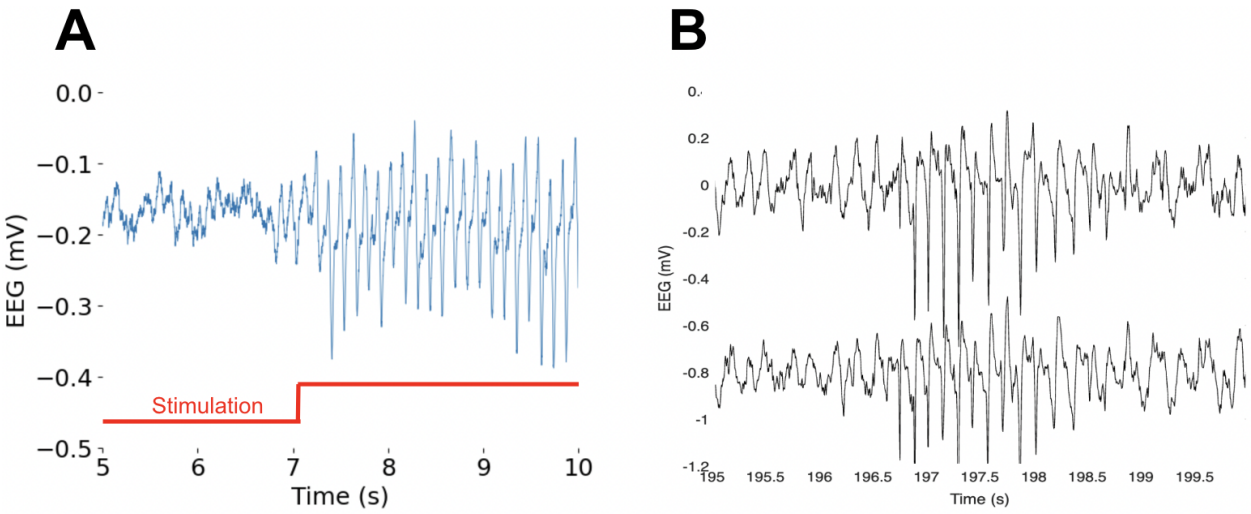

Figure 12: **Comparison of computational and biological EEG data**

(A) Computational EEG simulation with thalamic and reticular thalamic stimulation applied from 7 second to 10 seconds elucidating seizure dynamics. Simulation shown is that of an excitatory somatosensory population. (B) Unpublished biological EEG recordings (Knowles lab, Stanford) of excitatory (top) and inhibitory (bottom) somatosensory cortical populations in a mouse model with seizure events occurring from approximately 196.5-198.5 seconds. Parameters used for this figure are summarized in Table 2. The code used to generate the figure can be found in Code 2

tational EEG data set and Figure 12B shows direct EEG recordings of seizure activity in a mouse model. The computational and biological data bear a striking resemblance, where oscillations take similar shape, amplitude, as well as frequency. The oscillatory frequency being quite similar is especially important, as it indicates that our model has properly constrained the biological parameters given by our research collaborators. Overall this indicates our biologically constrained model to be a relevant representation of neural activity happening in vivo.

3.4 Results

The results in this chapter will take two main forms. The first being use of our bihemispheric model in order to compare and contrast computational results with those recorded by our research partners (Knowles Lab, Stanford) in vivo. This allows for validation of our model through experimental results, as well as confirmation of said results. These findings will also quantify the effect of changing callosal myelination on the thalamocortical network, thus providing further insight on how ADM influences seizure dynamics such as spectral properties. The second type of results are those aimed at uncovering specific physical mechanisms involved in trends found during the contrast between biological and computational data sets.

Reproducing in vivo results

Different seizure types have their own spectral fingerprint. Depending on the host parameters, such as tract lengths or conduction velocities, each seizure will give rise to different peak frequencies and powers that provide insight into the effect of ADM on seizure dynamics. This fingerprint is also strong method of contrasting computational with biological results, as similar spectral properties indicate validity of the computational model, and thus in turn verify the results recorded in vivo. The methodology of our research partners includes comparison of the Scn8a mouse model at high and low conduction velocities. The Scn8a mouse model has a mutation in the voltage gated sodium channel gene Scn8a, result-

ing in epilepsy presentation and absence seizures, making it a strong model for the questions at hand. The differential conduction velocities are brought about using an oligodendrocyte precursor knockout line, which prevents ADM and results in mice with distinct callosal conduction velocities [2]. Since much of the biological research being contrasted is unpublished, it will not appear in the thesis, however descriptions of the data will be included to explain the similarities and differences between the computational and biological models. It is important to note that our model is informed by recordings made by collaborators in Scn8a mice, as it relates to tract lengths, conduction velocities, and conduction delays. The first comparison we will make is between the power spectral densities of the two models. In the mouse model, we have a case of high myelination, resulting in a CV of approximately 1.5 m/s (Scn8a++/mut), and a case of low myelination, with an associated CV of 0.5 m/s (Scn8a++/mut OPC cKO). The case of high myelination results in peak ictal power occurring at approximately 8Hz, thus lying within the theta band which is commonly seen in mouse models of absence seizure activity [2] . The case of low CV, however, presents with a peak that is shifted slightly towards a higher frequency of 8.5Hz, indicating lower callosal CV to result in slightly higher frequency of oscillation. More striking is the contrast between peak spectral powers, where high CV mice show a peak spectral power approximately 2.5 times that of low CV mice, indicating far bigger oscillations in mice with high callosal CV.

These trends seen in biological data are seemingly robust, as they are reproduced by our independent computational model recordings. As seen in Figure 13A, peak frequencies remain in the 8-8.5Hz range for our model. Importantly, the low CV (representing less myelin) simulations also show the slight shift to higher oscillatory frequency, as well as substantial decreases in peak spectral power, emulating the results seen in biological recordings.

Another important marker of similarity between biological and computational models comes in the form of inter-hemispheric coherence. Coherence is a measure of the correlation between two signals as a function of frequency, reflecting how well one signal can predict another. In the context of EEG, coherence assesses the synchronization between

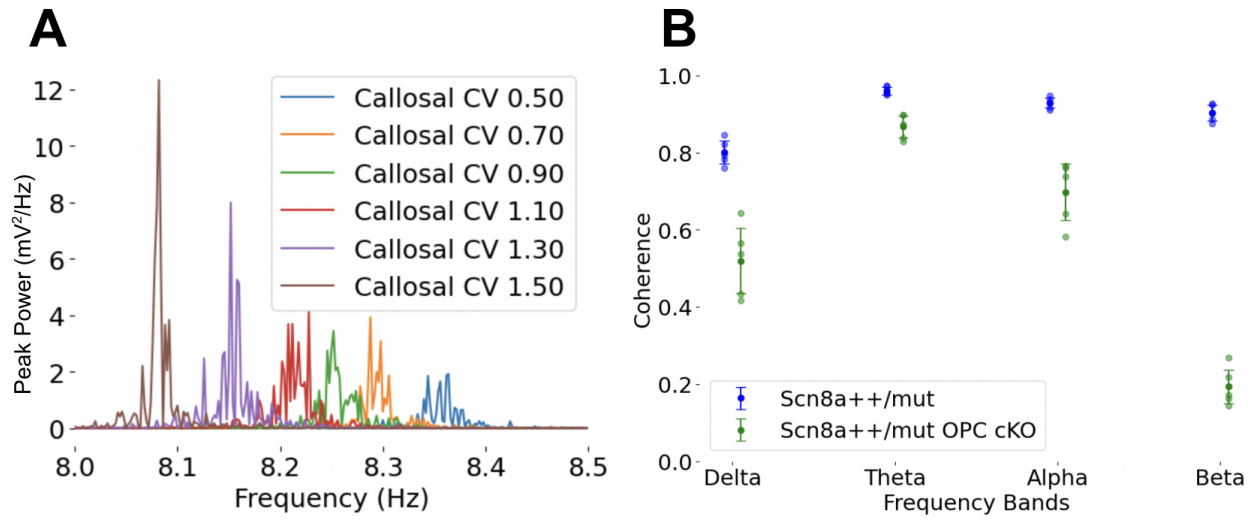

Figure 13: **Power spectral density of absence seizures at different callosal CVs**

(A) Power spectral density of oscillatory activity during computational seizure event at different callosal conduction velocities. (B) Coherence between hemispheres during computational seizure event at high (1.5m/s)(blue) and low (0.5m/s)(green) conduction velocities across frequency bands. Parameters used for this figure are summarized in Table 2. The code used to generate the figure can be found in Code 2

signals recorded from different brain regions. High inter-hemispheric coherence indicates strong connectivity and synchronous activity between the two hemispheres. In terms of seizure progression, changes in coherence can reveal how seizures affect brain connectivity and the dynamics of neural networks, helping us understand the spread and impact of absence seizures in thalamocortical networks. High levels of coherence at any CV implies cross talk between hemispheres, and potentially suggests a mechanism by which seizures can be amplified through a resonance like phenomenon [87] [88]. Furthermore, when comparing coherence at different CVs, we can confirm and begin to understand the effect of increased callosal myelination on inter-hemispheric dynamics. In biological recordings provided by our research partners, coherence in the delta, theta, alpha, and beta frequency bands were higher in cases of increased callosal myelination, whereas there was a marked decrease when oligodendrocyte precursor cells were knocked out (OPC cKO) and ADM was blocked. This contrast proposes higher callosal myelination states as a method of increased neural synchrony between hemispheres. These results were in agreement with our computational models, as seen in Figure 13B, where the OPC cKO condition (CV = 0.5m/s) had a marked decrease in coherence in each frequency band relative to the non knockout (CV = 1.5m/s) condition. Importantly, the non-theta band coherence may be a product of harmonics of pathological oscillations occurring in the theta band, resulting in similar trends being visualized in other frequency bands. Overall, these results not only validate our model as an accurate representation of neural activity, but also provide a hint as to the mechanism for increased seizure severity with respect to increased callosal myelination. The mechanism we will argue for is that of resonance, whereby increased myelin reduces callosal delays, allowing interhemispheric populations to interlock and amplify each other causing the increases in peak spectral power we see in Figure 13A.

Underlying Mechanism

Resonance is a physical phenomenon whereby a system oscillates at increasing amplitudes at a given frequency, often known as its natural frequency [89]. The increase in amplitude is derived from an external influence which also oscillates at the systems natural frequency, thus increasing the activity within the system. It can be easily understood when thinking of a swing, where pushing the swing at its natural frequency leads to an increase in height reached with each push. While certain examples of resonance are harmless, others are less so; earthquakes with oscillatory behaviour matching that of buildings can cause severe damage to infrastructure, and in the case of the brain, resonance inducing hyperactivity and strong oscillations suggest a potential pathology for seizure activity.

Within the computational bihemispheric model, we hypothesize that resonance may explain certain trends we see in our results, as well as those seen in biological samples [2]. One of the important observations we make relates to peak spectral powers at different callosal CVs, where higher CVs resulted in increased peak spectral power during oscillatory activity, as seen in Figure 13A. The stark increase in amplitude suggests communication between the two hemispheres as a driver of oscillatory activity, and the shift in natural frequency of the system begins to suggest resonance between the thalamocortical circuits found in each hemisphere. As previously mentioned, similar oscillatory frequencies are essential to create resonance within a system, and as shown in Figure 13B, the coherence in oscillatory activity between the two hemispheres increases drastically at higher CVs. Furthermore, they reach their peak coherence in the alpha and theta frequency bands, which represent the pathological oscillations within our system. The increased levels of coherence at higher callosal CVs, in conjunction with greater oscillatory amplitudes during seizure events, presents a strong case for resonance as the mechanism for why higher CVs result in greater seizure activity.

It is important, however, to ensure that the levels of coherence and increased power are indeed a result of cross talk between excitatory somatosensory cortical populations, and not just a coincidence resulting from concurrent stimulation of both hemispheric thalamic

populations used to trigger seizure onset. In order to investigate this we stimulated one hemisphere while recording activity in both hemispheres to see the contralateral influence at play. This experiment is shown in Figure 14A, where recordings of both right and left hemispheres are shown, while only the left hemisphere is stimulated. The recording illustrates seizure generalization from the left to right hemisphere, after stimulation began at 2 seconds. The contrast in activity shows us that coherence between hemispheres at high CVs is indeed a result of the differential interplay with lower callosal delays, as the two hemispheres begin to cohere as a result of single hemisphere stimulation. Furthermore, it provides some insight into the underlying mechanism; at approximately 3 seconds, the right hemisphere begins to experience some pathological oscillations, and right after that point, the oscillations within the left hemisphere begin to rise in amplitude, indicating a scheme of resonance whereby each hemisphere induces an increase in oscillatory behaviour to its contralateral counterpart. It is, however, important to further numerically quantify this interlocking of the two hemispheres, as it brings about a more concrete link between resonance and the generalization of seizure activity we observe. This was done by creating a spectrogram of the EEG data, which will derive the natural frequencies of each hemisphere, thereby supporting our hypothesis of resonance if these natural frequencies align.

The natural frequencies of each hemisphere do in fact align, as seen in Figure 14B where the highest intensity of oscillatory frequencies for both hemispheres falls right around 8Hz. This aligns with the oscillatory frequency elucidated in previous modelling efforts which used thalamic stimulation in both hemispheres, as well as experimental recordings taken by our research partners. The results also align temporally, whereby the strongest and most intense oscillatory activity appears at the same time in the EEG recordings of each hemisphere, as well as their associated spectrograms. The spectrogram also illustrates a transition period for the left hemisphere at stimulation onset, where it climbs to its natural frequency, and once reached, begins the process of generalization. Generalization is the spread of seizure activity from one area, such as a focal zone, to other parts of the brain [90]. One type

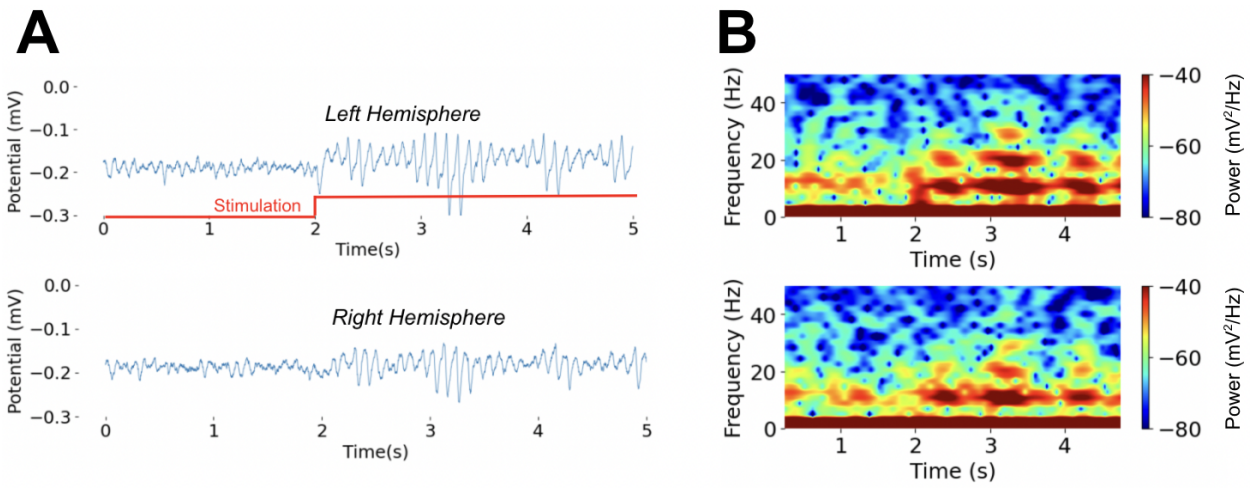

Figure 14: **Spectrogram's and EEG's of absence seizure activity resulting from uni-hemispheric stimulation**

(A) EEG recordings of right and left excitatory pyramidal populations with stimulation applied to the left hemisphere's thalamic populations at 7 seconds. (B) Spectrogram's illustrating the intensity of oscillations at each frequency between 0-50Hz during the time series presented in (A). Parameters used for this figure are summarized in Table 2. The code used to generate the figure can be found in Code 2

is bilateral generalization, where seizure activity in one hemisphere spreads across callosal tracts, inducing a seizure event in the other hemisphere. This idea of generalization is significant, as our results Figure (14) show the non-stimulated hemisphere (right) to only start oscillating with high intensity once the stimulated hemisphere (left) has reached its natural frequency, thus allowing resonance to occur, and the seizure to generalize to the right hemisphere after a brief conduction delay. Additionally, the generalization further intensifies oscillation in both hemispheres, where highest magnitudes are seen once this process has occurred. Further illustrating the amplification effect of resonance within the system. Note that one can also observe higher harmonics at multiples of the oscillatory frequency.

Influence of CV on Resting State Dynamics

While we hypothesize resonance to be the mechanism underlying our results, we must still characterize how resonance influences the dynamics of our model. In chapter 2, we measured variance in firing rate relative to CV. The results, shown in Figure 10, describe a system where increasingly variable firing activity results from increases in CV and noise amplitude. This provides a strong candidate mechanism for the trends seen in the bihemispheric model, as well as certain data seen in experimental recordings not investigated by our model. In order to evaluate the validity of this claim, we quantified the variance in callosal firing rate, meaning the contralateral firing rate of pyramidal populations, without stimulation and relative to callosal CV. The result, pictured in Figure 15A, shows that variance in firing rate increases with callosal CV, indicating that increased seizure burden results from larger amplitude fluctuations in firing rate, reflected by increased variance, matching our results in Chapter 2 (Figure 10). The mean callosal activity, however, remained stable, implying variance as the causal factor for the shift from lesser to greater oscillatory activity during seizure events, also similar to results pictured in Figure 10.

The bihemispheric model we have constructed does not measure seizure rate, as the seizures are deliberately provoked through thalamic stimulation, meaning it would not pro-

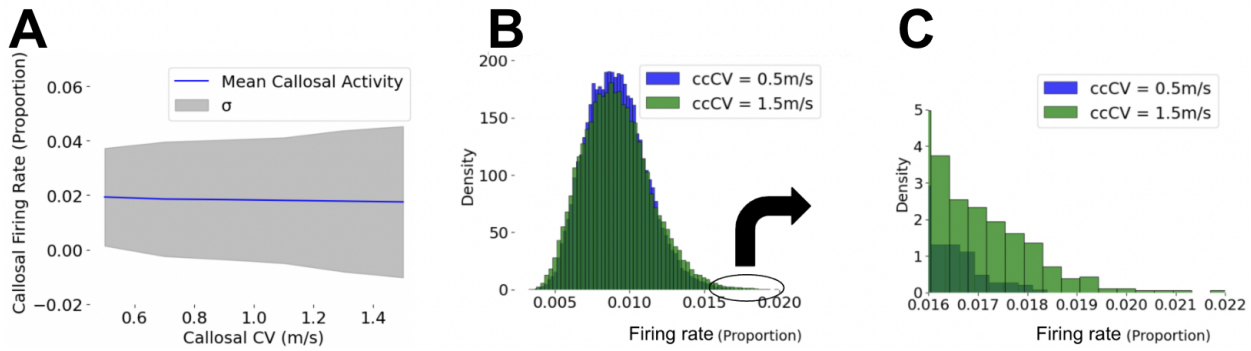

Figure 15: **Variance in callosal firing rate, and firing rate histogram during non seizure state activity**

(A) Callosal firing rate relative to callosal CV (ranging from 0.5m/s - 1.5m/s) with standard deviation in firing rate during non-oscillatory (non-stimulated) activity (B) Histogram of firing rates during non-oscillatory activity at different callosal CVs (C) Enlarged section of (B) showing relative contribution of each CV at high firing rates. Parameters used for this figure are summarized in Table 2. The code used to generate the figure can be found in Code 2

vide any further insight. Our research partners did however measure this in mouse models, and unsurprisingly found an increase in seizure rate at higher callosal CVs. This finding is supported by our investigations shown in Figure 15B/C surrounding firing rate during non-seizure state (transient) activity. Our results illustrate an increase in firing rate variance during transient activity, and more instances of very high firing rates when the callosal CV is increased. Since high firing rates push the system closer to a bifurcation point, this likely results in a higher seizure rate, which is confirmed in experiments done by research partners.

Corpus Callosotomy

Severing the connection between hemispheres of the brain is referred to as a corpus callosotomy, and is a procedure used to alleviate symptoms in patients with intractable epilepsy [91]. In our model, bilateral callosal firing rate is clearly affected by callosal CV, and is also affected by the synaptic weight parameter, Wcc in equation 14, pertaining to the callosal weighting.

By changing Wcc, we should be able to alter the coupling between hemispheres to see how it impacts seizure activity in each hemisphere, as well as showcase how resonance is involved. This reproduction would isolate changes in contralateral pyramidal neuron firing as the reason for changes in spectral characteristics and activity in our model, thus strengthening our hypothesis. Furthermore, a lack of connection between hemispheres would in essence reproduce the effects of a corpus callosotomy. Therefore, this investigation would not only further our hypothesis, but also illustrate the predictive capabilities of this model, as it emulates neural activity seen before and after a surgical procedure, despite not being constructed for this purpose. In Figure 16A we see the effect of computationally severing the connection

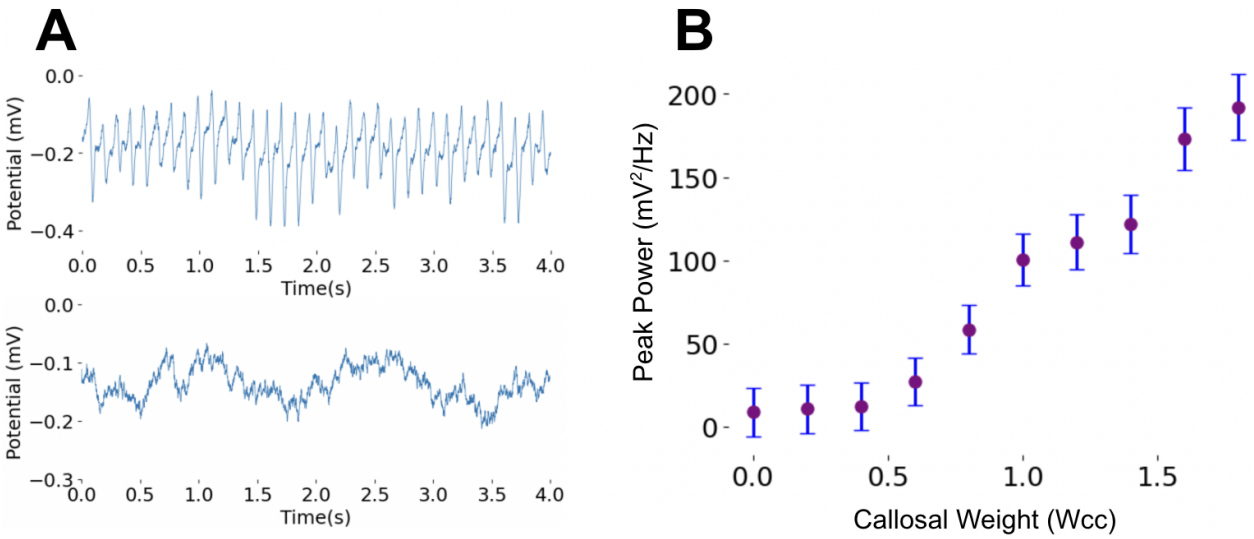

Figure 16: **Computational EEG recordings of a corpus callosotomy with peak spectral powers at differing levels of callosal synaptic weight during thalamic stimulation**

(A) Two distinct time series of membrane activity in the excitatory population of the somatosensory cortex at callosal weights of 0 (bottom), and 1.5 (top) (B) Peak spectral power of seizures at different callosal weights (ranging from 0 - 1.8). Parameters used for this figure are summarized in Table 2. The code used to generate the figure can be found in Code 2

between hemispheres, where a callosal weight of $Wcc = 0$ fully suppresses epileptiform activ-

ity, despite the constant thalamic stimulation. This effect is reversed when the connection is reestablished with a callosal weight of $Wcc = 1.5$, and seizure activity reemerges throughout the time series with constant thalamic stimulation. Previous discussion surrounding verification of bilateral firing input comes to fruition in Figure 16B, where peak spectral powers of oscillation are compared at different callosal weights. The trend observed illustrates increasing callosal weight, and thus increasing bilateral input, to augment the peak spectral powers observed during seizures, thus indicating strength of cross-talk between hemispheres as the causal numerical mechanism for greater seizure burden in our bihemispheric model.

3.5 Discussion

Overall, our goal throughout this chapter has been to use computational methods to reproduce the effect of differing myelination patterns in bihemispheric thalamocortical circuits, to create an understanding surrounding ADM and seizure dynamics. We expanded our investigation to elucidate a potential mechanism for the observed results, and found resonance to be a suitable candidate. We hypothesize that higher levels of myelination, yielding greater CV, allows for greater coherence between hemispheres, triggering resonance amplifying seizure dynamics both within and between hemispheres.

The investigation began with comparisons between our data, and the biological recordings provided by our research partners. Qualitatively, our EEG data took on very similar characteristics to EEG's in Scn8a mouse models. Since we used their recordings of distances and delays to inform our model, qualitatively similar recordings indicate that our model is doing well to encompass the membrane activity seen in vivo. While our model passed the eye test, it was important to provide more numerical and objective comparisons in order to validate its use. This was accomplished with recordings of spectral characteristics, which were then compared with spectral recordings of biological activity to confirm the models ability to encapsulate core features of seizure events. In biological recordings, peak spectral power during seizure events was found to be approximately 2.5 times higher in cases of high

CV (1.5m/s) versus cases of low CV (0.5m/s). Meaning that increased myelination results in stronger oscillatory activity during seizures. These results were robust in our computational model, whereby lower callosal CVs yielded much smaller peak spectral powers during seizure events as illustrated in Figure 13A. Furthermore, peak frequencies in both biological and computational recordings showed a slight shift with altered callosal CV, where an increase in CV seemingly reduced the associated peak frequency. This result not only provided further support to our models validity, but also hinted at a potential underlying mechanism. Resonance is a phenomena where two oscillators with the same natural frequency can become in phase, resulting in amplification of their signals. The natural frequency of a system can be dependent on a number of factors, however within our system, greater callosal CV seems to alter natural frequency, and along with this comes an increase in peak spectral power. This correlation suggests resonance between hemispheres as a potential mechanism behind increased seizure severity with increasing callosal CV.

In order to propose resonance as the mechanism underlying shifts in seizure dynamics relating to ADM, we will use results given by the thalamocortical model as arguments for its influence. The first question to answer related to differences in oscillatory activity. More specifically: why does increasing callosal CV create a stronger resonance effect? This question is partially answered in Figure 13B, where we measure coherence between excitatory somatosensory populations in the case of high (1.5m/s) and low (0.5m/s) callosal CV. A higher level of coherence indicates two oscillators to be more in phase, and when they are more in phase, a greater amplification effect precipitates. This can be understood using the swing example of resonance, where giving a push at the maximum height, which is akin to being in sync, yields a greater peak height relative to a push coming before or after the swing reaches its peak. Using this understanding, we see greater coherence in all frequency bands of high callosal CV seizure events as a potential explanation for why larger oscillations occur, as the two oscillators (excitatory somatosensory populations) are far more in sync and thus producing greater resonance effect.

While we are starting to see how resonance could contribute to the results seen in both computational and biological models, it is important to confirm its involvement through additional means. One such way is by examining an EEG time series with only one hemisphere experiencing stimulation. In this case, seeing pathological oscillations in both hemispheres would illustrate the ability of each hemisphere to induce oscillatory activity onto the other. This is shown in Figure 14A, where stimulation in the thalamic populations of the left hemisphere induces seizure activity in the right hemisphere. Furthermore, once oscillatory activity presents in the right hemisphere, oscillations in the left hemisphere begin to increase in amplitude, directly illustrating the resonance effect in our model. Spectrograms provide a way to objectively evaluate the intensity of different frequencies during an EEG time series. Figure 14 provides a 5 second EEG recording in the excitatory somatosensory population of both hemispheres with stimulation being applied to the left hemisphere at 2 seconds. It also provides the associated spectrogram of these recordings. Of critical importance is the activity occurring right as stimulation is applied, where our spectrograms illustrate greater intensity between 0-10Hz during the first 200ms or so in the left hemisphere. This rise in intensity is however not present in the right hemisphere, and the increased intensity in the right hemisphere is only seen once the left hemisphere reaches its stable natural frequency near 8-9Hz. These results directly illustrate the schema of resonance, where two oscillators are in phase at their natural frequency and amplify each other. Furthermore, the strongest oscillations in the left hemisphere only occur once the right hemisphere is also oscillating around 8-9Hz, clearly showing the mechanism underlying increased seizure dynamics to be resonance in our model. Overall, these results provide a mechanism, not only for our model, but also for phenomena observed in mouse models where seizure severity is positively correlated with callosal myelination and thus CV.

We now have an explanation as to why we see specific trends in our model relating to spectral characteristics and qualitative features, however it is also important to elucidate the underlying numerical cause for said effects. In chapter 2 we saw variance to be the reason

for increased seizure burden, making it a logical parameter to quantify and investigate for its role in resonance amplified seizure dynamics. With increased peak spectral powers at higher callosal CVs, an increase in variance of firing within the callosal tracts would provide a numerical mechanism behind the trend. This is because greater variance in firing indicates a way by which membrane activity could be influenced to oscillate with greater amplitude. We do infact see this in Figure 15A, where greater callosal CVs are associated with higher degrees of variance in callosal firing rate, indicating this trend as the numerical explanation for resonance implementation in the model. Importantly, mean callosal activity does not change significantly with callosal CV, which isolates variance as the cause, since a change in mean activity would have also potentially explained our results. While the bihemispheric model relies on stimulation to induce seizure activity, thus eliminating relevance of seizure rate, our research partners measured it in vivo and found it to be higher in cases of greater callosal myelination. This trend is also likely explained by variance in callosal firing rate, whereby greater firing rates push the system closer to its bifurcation point yielding seizure events more often. In order to verify this idea, we characterized the firing rates present in cases of high (1.5m/s) and low (0.5m/s) callosal CV during transient activity. As pictured in 15B/C, greater CV results in a distribution of firing rates with more variance, meaning it disproportionately presents extreme values, such as those hypothesized to induce seizure events, relative to a system with lower callosal CV. This is best shown in Figure 15C, where the extreme firing rates ranging from 0.016-0.022 (proportion firing) occur far more often in the high CV case. Not so coincidentally, this range of firing rates coincides with the mean callosal firing rate during seizure events of approximately 0.02, further supporting the idea of greater variance at high CVs yielding higher firing rates that make the transition to a seizure state far easier. Overall, these results illustrate the numerical perspective within the model that explains how resonance effects the system at differing CVs, allowing for contrasting spectral characteristics, and increased seizure burden.

While the case for differing callosal firing rates underlying resonance, and thus seizure

activity, within our system is strong, further investigations can cement it as the numerical mechanism. In our model, callosal weight can modulate bilateral firing input between hemispheres, thus providing an alternative way to confirm callosal firing as reason for differing seizure dynamics. Luckily, biological investigations similar to this have been done in the past, whereby callosal connections have been severed surgically to alleviate symptoms in forms of epilepsy not respondent to traditional treatments [91]. With this in mind, a reduction in callosal weight should reduce spectral characteristics such as peak spectral power, and reduce oscillatory activity in the system. This is infact what we see in Figure 16A, where eliminating the callosal connection with a $Wcc = 0$, moves the system from a paradigm of seizure activity, back to regular asynchronous activity seen in a healthy brain. While modulation of the callosal connection in humans, unsurprisingly, has many unintended consequences making it a last resort, the computational contrast illustrates bilateral firing as the numerical mechanism underlying increased seizure activity with increased callosal myelination. Figure 16B further illustrates this idea, whereby an increase in callosal weight has a direct positive relationship with peak oscillatory power, meaning greater bilateral firing results in strong oscillations and seizure dynamics.

In conclusion, we postulate that increased seizure dynamics are associated with greater callosal conduction velocities, resulting from greater callosal myelination, and can be explained by resonance between somatosensory cortices. The resonance effect is then amplified at greater callosal CVs, as it allows for the two oscillators to become more in phase, and creates a system more inclined to seize as it is more easily pushed to the edge of a bifurcation point towards a seizure. Lastly, markers of seizure intensity such as peak spectral power are then magnified by resonance between hemispheres, creating a system not only more inclined to seize, but to do so more dramatically resulting in greater seizure burden due to an increase of myelin along the corpus callosum.

Chapter 4

Discussion

4.1 Chapter Summary

In this chapter we start with a discussion of the scientific implications of our research. We then follow up with potential future research that can be done to build upon our work. Lastly, we summarize the thesis and add some final thoughts regarding our research.

4.2 Scientific Implications

The results elucidated through our Wilson-Cowan investigations answer many questions, and open the door for many more. We show, through computational methods, that increased CV, a proxy for myelination in callosal tracts, yields greater seizure burden within thalamocortical networks. Whereby faster signal transmission causes higher levels of correlation between inputs, thus opening the door for larger amplitude fluctuations as there is no diversity associated stabilizing factor in the input potentials. Encouragingly, our research collaborators have found similar trends in mouse models, where greater callosal myelination, caused by ADM, results in higher absence seizure frequency, and alterations in spectral markers for seizure burden such as peak spectral power [2]. We further this research by not only reproducing the biological data sets using computational means, but also proposing candidate mechanisms for the associated trends. The primary mechanism proposed being that of resonance. In the thalamocortical network, we have paired oscillators between hemispheres, and reductions in conduction delays between the oscillators results in greater coherence and thus greater resonance as the oscillators are more in phase. The increased severity of seizure states results in more myelin through ADM, outlining a positive feedback loop in which myelin and seizures work together to cause significant epilepsy progression.

The idea that resonance and glial cells are involved in epileptogenesis is quite novel, making investigations into the specific pathologies involved very exciting as it opens up avenues for new therapeutics with potential to significantly decrease the disease burden of those with epilepsy. Through our investigations, thalamocortical networks become potential targets for pharmaceutical or surgical interventions, particularly in cases of progressive epilepsy as-

sociated with white matter plasticity. Using this framework we hope to contribute to the reduction of disease burden imposed by epilepsy. Furthermore, our research can hopefully act as a proof of concept, where computational models investigating ADM can be used to research other diseases potentially affected by myelination patterns, such as Alzheimer's Schizophrenia, Multiple Sclerosis or any other relevant disease [92] [93] [94]. Using these methods can provide a much quicker, and much less expensive, way to answer certain questions, as well as guide future experimentation resulting in a more streamlined and efficient way of conducting research pertaining to neurological disease.

4.3 Future work

While our work has brought about new insights, it has also brought about new questions and the need for further investigation. Whether it be adjusting the model to better fit the phenomena of ADM, understanding influences of different neural tracts, or constructing a new model that can delve into the problem on a different scale, there are many paths that have been opened for future work.

The implementation of Wilson-Cowan equations in our model saw adjustment of CV as a proxy for myelinatory state. While we have argued this to be a valid method for understanding ADM, it somewhat omits the procedural part, instead giving a cross-sectional view as opposed to a dynamic model replicating the changes to myelination in real time. In future iterations of the bihemispheric model, it may be prudent to include changes to the CV as a response to seizure events in real time. Using previously discussed methods of seizure detection, we could construct a version in which the positive feedback loop of seizures and myelination is on full display, creating a more holistic version that is easier to contrast with biological data sets. The one limiting factor in this proposed iteration revolves around simulation time, as the time scales would have to be condensed in computational models to not take significant amounts of time for a single simulation.

Other questions have been posed by our collaborators, in terms of ADM specificity in

different thalamocortical tracts. Throughout their research they have found ADM in callosal tracts, however in the connections between the somatosensory cortex and the thalamic populations, otherwise known as the internal capsule, myelination is quite stable despite seizure propagation through these tracts. A new avenue could thus be explored, in which dynamics at altered capsule myelination states could be derived computationally, hopefully producing some insight into why there is no ADM along these tracts. Alternatively, these tracts may require stability from a myelination perspective for proper function of unrelated neural systems. Either way, our computational methods allow investigation otherwise difficult in vivo, due to the stable nature of these tracts in vivo.

While we see how computational methods can answer certain questions difficult for biological investigations, the inverse is also true. For example, our model only includes CV as a proxy for myelination, however there may be other factors at play as well. It is entirely possible that myelin has other effects on the neural dynamics we model, however this is a question that can be difficult to answer computationally and must be investigated using experimental methods. Doing experiments in vivo trying to understand what other influences myelin could have would be important in either elucidating other explanations, or further supporting our assumption of CV as a proxy for myelination. These investigations could revolve around specific delay timing seen in animal models, or could elucidate other myelin related molecular mechanisms potentially contributing to the pathological understanding of absence seizure progression. Overall, while we have brought about important insights through computational modelling, using other methods of investigation in conjunction would be important in providing a holistic understanding of the progressive absence seizure pathology as a whole.

4.4 Final Thoughts

We start the thesis with an outline of Wilson-Cowan modelling, and by illustrating the importance of neural heterogeneity as a protective factor against seizure dynamics. Our research continues through the alteration of the Wilson-Cowan model to include conduction

delays, allowing for inquiries into neural dynamics relative to CV, which acts as a proxy for myelination. This investigation led to the understanding that increased myelination could result in greater seizure burden, in terms of both frequency and spectral properties. We next built a bihemispheric model in order to compare and contrast computational methods with observations made in Scn8a mouse models by our collaborators (Knowles Lab, Stanford). Their research illustrated a motif whereby absence seizures originating in a bihemispheric thalamocortical network increased myelination along the corpus callosum which connects the brains hemispheres. This increase in myelination then resulted in greater seizure burden, thus outlining a positive feedback loop of seizure progression. Our results replicate their findings in terms of spectral properties, and further the research by proposing resonance as a candidate mechanism for myelin induced bihemispheric seizure dynamics. Taken together, our findings illustrate a novel target for future therapeutics, hopefully reducing the burden of epilepsy, specifically in the developmental absence seizure pathology often seen in children afflicted with the disease [2]. The research also provides a bihemispheric framework based on Wilson-Cowan equations which can be used in order to answer a wide variety of questions regarding whole brain dynamics, providing an inexpensive computational model which can also guide future experimentation in biological models.

Appendix

Parameters	Values	Description
V_n	Varies (mV)	Membrane potential
h_n	Varies (a.u.)	Excitability threshold
β	4.8 (a.u.)	Neuronal response gain
τ	Varies (ms)	Axonal conduction delay
CV	Varies (m/s)	Axonal conduction velocity (CV; unspecific)
w_{PYRPYR}	2.7 (a.u.)	Baseline PYR PYR synaptic weight
w_{PYRIN}	1.5 (a.u.)	Upper bound on PYR IN synaptic weights
w_{INPYR}	-2.8 (a.u.)	Baseline IN PYR synaptic weight
w_{ININ}	0 (a.u.)	Upper bound on IN IN synaptic weights
dt	1 (ms)	Time step
D	0.00005 (mV)	Baseline noise amplitude
$\alpha_P YR$	100 (Hz)	Excitatory rate constant
$\alpha_I N$	100 (Hz)	Inhibitory rate constant
$\sigma_P YR$	Varies (mV)	Excitatory heterogeneity
$\sigma_I N$	Varies (mV)	Inhibitory heterogeneity
$\epsilon_P YR$	Varies (mV)	Excitatory independent gaussian white noise
$\epsilon_I N$	Varies (mV)	Inhibitory independent gaussian white noise
l	Varies (mm)	Axonal length

Table 1: Summary of model parameters for Chapters 1 and 2, symbols and variables. Detailed information are provided in figures' caption as well as in source codes.

Parameters	Values	Description
β	25 (a.u.)	Neuronal response gain
$\tau_{callosal,k}$	Varies (ms)	Callosal conduction delay
τ_{CT}	5 (ms)	Cortico-thalamic conduction delay
c_k	Varies (m/s)	Callosal conduction velocity
$w_{callosal}$	1.5 (a.u.)	Baseline callosal synaptic weight
$w_{PYR,PYR}$	0.9 (a.u.)	Baseline PYR,PYR synaptic weight
$w_{IN,PYR}$	-2.2 (a.u.)	Baseline IN,PYR synaptic weight
$w_{IN,IN}$	-0.5 (a.u.)	Baseline IN,IN synaptic weight
$w_{PYR,IN}$	1.5 (a.u.)	Baseline PYR,IN synaptic weight
$w_{VB,RTN}$	1.44 (a.u.)	Baseline VB,RTN synaptic weight
$w_{RTN,VB}$	-1.6 (a.u.)	Baseline RTN,VB synaptic weight
$w_{PYR,VB}$	1.9 (a.u.)	Baseline PYR,VB synaptic weight
$w_{PYR,RTN}$	2 (a.u.)	Baseline PYR,RTN synaptic weight
$w_{VB,PYR}$	1.5 (a.u.)	Baseline VB,PYR synaptic weight
$w_{IN,IN}$	1.8 (a.u.)	Baseline IN,IN synaptic weight
dt	1 (ms)	Time step
α_{PYR}	10 (Hz)	Excitatory pyramidal rate constant
α_{IN}	10 (Hz)	Inhibitory interneuron rate constant
α_{VB}	1 (Hz)	Ventrobasal rate constant
α_{RTN}	0.5 (Hz)	Reticular thalamic rate constant
ϵ_θ	Varies (mV)	Observational independent gaussian white noise
$\epsilon_m^{r,l}$	Varies (mV)	Independent gaussian white noise
l	Varies (mm)	Axonal length
$V_m^{r,l}$	Varies (mV)	Membrane potential
$B_P^{r,l}YR$	-0.5 (mV)	Baseline PYR current
$B_I^{r,l}N$	-0.6 (mV)	Baseline IN current
$B_V^{r,l}B$	-0.15 (mV)	Baseline VB current
$B_R^{r,l}TN$	-0.5 (mV)	Baseline RTN current
$S_P^{r,l}YR$	0 (mV)	Stimulating PYR current
$S_I^{r,l}N$	0 (mV)	Stimulating IN current
$S_V^{r,l}B$	0.0525 (mV)	Stimulating VB current
$S_R^{r,l}TN$	0.0525 (mV)	Stimulating RTN current
D_PYR	0.00001 (mV)	Baseline PYR noise amplitude
D_IN	0.00001 (mV)	Baseline IN noise amplitude
D_VB	0.0000001 (mV)	Baseline VB noise amplitude
D_RTN	0.0000001 (mV)	Baseline RTN noise amplitude

Table 2: Summary of model parameters for Chapter 3, symbols and variables. Detailed information are provided in figures' caption as well as in source codes.

Coding Specifics

Local network model [Code 1] code found at: https://colab.research.google.com/drive/1vx5_ZuTgbrl8cP5ZtAPVFFVK3yAExCiB?usp=sharing Bihemispheric model [Code 2] code found at: https://colab.research.google.com/drive/1lkWDbAyaXFCfx1qgOvb0JT6FLXUvmKIn?usp=sharing Specific values can change according to the investigation, however these are the frameworks used for each model.

References

[1] Ettore Beghi. The epidemiology of epilepsy. *Neuroepidemiology*, 54(2):185–191, 2020.

[2] Juliet K Knowles, Haojun Xu, Caroline Soane, Ankita Batra, Tristan Saucedo, Eleanor Frost, Lydia T Tam, Danielle Fraga, Lijun Ni, Katlin Villar, et al. Maladaptive myelination promotes generalized epilepsy progression. *Nature Neuroscience*, 25(5):596–606, 2022.

[3] Scott Rich, Homeira Moradi Chameh, Jeremie Lefebvre, and Taufik A Valiante. Loss of neuronal heterogeneity in epileptogenic human tissue impairs network resilience to sudden changes in synchrony. *Cell reports*, 39(8):110863, 2022.

[4] Charles F Stevens. The neuron. *Scientific American*, 241(3):54–65, 1979.

[5] Nelson Spruston. Pyramidal neurons: dendritic structure and synaptic integration. *Nature Reviews Neuroscience*, 9(3):206–221, 2008.

[6] Henry Markram, Maria Toledo-Rodriguez, Yun Wang, Anirudh Gupta, Gilad Silberberg, and Caizhi Wu. Interneurons of the neocortical inhibitory system. *Nature reviews neuroscience*, 5(10):793–807, 2004.

[7] Desdemona Fricker and Richard Miles. Epsp amplification and the precision of spike timing in hippocampal neurons. *Neuron*, 28(2):559–569, 2000.

[8] Heather Lynne Gilmour, Paméla Louise Ramage-Morin, and Suzy L Wong. *Epilepsy in Canada: prevalence and impact*. Statistics Canada, 2016.

[9] Doru Georg Margineanu. Epileptic hypersynchrony revisited. *Neuroreport*, 21(15):963–967, 2010.

[10] JR De Kruijk, A Twijnstra, and P Leffers. Diagnostic criteria and differential diagnosis of mild traumatic brain injury. *Brain Injury*, 15(2):99–106, 2001.

[11] Jerome Engel Jr. Introduction to temporal lobe epilepsy. *Epilepsy research*, 26(1):141–150, 1996.

[12] Renzo Guerrini, Carla Marini, and Carmen Barba. Generalized epilepsies. *Handbook of clinical neurology*, 161:3–15, 2019.

[13] Sandra Kammerman and Lloyd Wasserman. Seizure disorders: Part 1. classification and diagnosis. *The Western journal of medicine*, 175(2):99, 2001.

[14] Malachy Bishop and Chase A Allen. The impact of epilepsy on quality of life: a qualitative analysis. *Epilepsy & Behavior*, 4(3):226–233, 2003.

[15] Mark A Kramer, Wilson Truccolo, Uri T Eden, Kyle Q Lepage, Leigh R Hochberg, Emad N Eskandar, Joseph R Madsen, Jong W Lee, Atul Maheshwari, Eric Halgren, et al. Human seizures self-terminate across spatial scales via a critical transition. *Proceedings of the National Academy of Sciences*, 109(51):21116–21121, 2012.

[16] Wilson Truccolo, Omar J Ahmed, Matthew T Harrison, Emad N Eskandar, G Rees Cosgrove, Joseph R Madsen, Andrew S Blum, N Stevenson Potter, Leigh R Hochberg, and Sydney S Cash. Neuronal ensemble synchrony during human focal seizures. *Journal of Neuroscience*, 34(30):9927–9944, 2014.

[17] Massimo Avoli, Marco De Curtis, Vadym Gnatkovsky, Jean Gotman, Rüdiger Köhling, Maxime Lévesque, Frédéric Manseau, Zahra Shiri, and Sylvain Williams. Specific imbalance of excitatory/inhibitory signaling establishes seizure onset pattern in temporal lobe epilepsy. *Journal of neurophysiology*, 115(6):3229–3237, 2016.

[18] Christopher D Makinson, Brian S Tanaka, Jordan M Sorokin, Jennifer C Wong, Catherine A Christian, Alan L Goldin, Andrew Escayg, and John R Huguenard. Regulation of thalamic and cortical network synchrony by scn8a. *Neuron*, 93(5):1165–1179, 2017.

[19] Zhihui Wang and Qingyun Wang. Eliminating absence seizures through the deep brain stimulation to thalamus reticular nucleus. *Frontiers in Computational Neuroscience*, 11:22, 2017.

[20] Ligia A Papale, Barbara Beyer, Julie M Jones, Lisa M Sharkey, Sergio Tufik, Michael Epstein, Verity A Letts, Miriam H Meisler, Wayne N Frankel, and Andrew Escayg. Heterozygous mutations of the voltage-gated sodium channel scn8a are associated with spike-wave discharges and absence epilepsy in mice. *Human molecular genetics*, 18(9):1633–1641, 2009.

[21] Kevin J Gaston and John I Spicer. *Biodiversity: an introduction*. John Wiley & Sons, 2013.

[22] Jerome Engel. Excitation and inhibition in epilepsy. *Canadian Journal of Neurological Sciences*, 23(3):167–174, 1996.

[23] Alexandros T Tzallas, Markos G Tsipouras, and Dimitrios I Fotiadis. Epileptic seizure detection in eegs using time–frequency analysis. *IEEE transactions on information technology in biomedicine*, 13(5):703–710, 2009.

[24] Christoph Baumgartner, Stefanie Lurger, and Fritz Leutmezer. Autonomic symptoms during epileptic seizures. *Epileptic Disorders*, 3(3):103–116, 2001.

[25] WH Theodore, RJ Porter, P Albert, K Kelley, E Bromfield, O Devinsky, and S Sato. The secondarily generalized tonic-clonic seizure: a videotape analysis. *Neurology*, 44(8):1403–1403, 1994.

[26] H Blumenfeld, GI Varghese, MJ Purcaro, JE Motelow, M Enev, KA McNally, AR Levin, LJ Hirsch, R Tikofsky, IG Zubal, et al. Cortical and subcortical networks in human secondarily generalized tonic–clonic seizures. *Brain*, 132(4):999–1012, 2009.

[27] Markos G Tsipouras. Spectral information of eeg signals with respect to epilepsy classification. *EURASIP Journal on Advances in Signal Processing*, 2019(1):1–17, 2019.

[28] Qi Yuan, Weidong Zhou, Liren Zhang, Fan Zhang, Fangzhou Xu, Yan Leng, Dongmei Wei, and Meina Chen. Epileptic seizure detection based on imbalanced classification and wavelet packet transform. *seizure*, 50:99–108, 2017.

[29] Masako Kaibara and Warren T Blume. The postictal electroencephalogram. *Electroencephalography and clinical neurophysiology*, 70(2):99–104, 1988.

[30] William Stacey, Michel Le Van Quyen, Florian Mormann, and Andreas Schulze-Bonhage. What is the present-day eeg evidence for a preictal state? *Epilepsy research*, 97(3):243–251, 2011.

[31] Chris Plummer, A Simon Harvey, and Mark Cook. Eeg source localization in focal epilepsy: where are we now? *Epilepsia*, 49(2):201–218, 2008.

[32] Luis Garcia Dominguez, Richard A Wennberg, William Gaetz, Douglas Cheyne, O Carter Snead, and Jose Luis Perez Velazquez. Enhanced synchrony in epileptiform activity? local versus distant phase synchronization in generalized seizures. *Journal of neuroscience*, 25(35):8077–8084, 2005.

[33] Udaya Seneviratne, Jia J Woo, Ray C Boston, Mark Cook, and Wendyl D'Souza. Focal seizure symptoms in idiopathic generalized epilepsies. *Neurology*, 85(7):589–595, 2015.

[34] CP Panayiotopoulos. Typical absence seizures and their treatment. *Archives of disease in childhood*, 81(4):351–355, 1999.

[35] Inseon Song, Daesoo Kim, Soonwook Choi, Minjeong Sun, Yeongin Kim, and Hee-Sup Shin. Role of the α1g t-type calcium channel in spontaneous absence seizures in mutant mice. *Journal of Neuroscience*, 24(22):5249–5257, 2004.

[36] Susumu Sato, Fritz E Dreifuss, and J Kiffin Penry. The effect of sleep on spike-wave discharges in absence seizures. *Neurology*, 23(12):1335–1335, 1973.

[37] O Carter Snead III. Basic mechanisms of generalized absence seizures. *Annals of Neurology: Official Journal of the American Neurological Association and the Child Neurology Society*, 37(2):146–157, 1995.

[38] Robert Stämpfli. Saltatory conduction in nerve. *Physiological reviews*, 34(1):101–112, 1954.

[39] David Purger, Erin M Gibson, and Michelle Monje. Myelin plasticity in the central nervous system. *Neuropharmacology*, 110:563–573, 2016.

[40] Michelle Monje. Myelin plasticity and nervous system function. *Annual review of neuroscience*, 41:61–76, 2018.

[41] Ethan G Hughes, Jennifer L Orthmann-Murphy, Abraham J Langseth, and Dwight E Bergles. Myelin remodeling through experience-dependent oligodendrogenesis in the adult somatosensory cortex. *Nature neuroscience*, 21(5):696–706, 2018.

[42] R Douglas Fields. A new mechanism of nervous system plasticity: activity-dependent myelination. *Nature Reviews Neuroscience*, 16(12):756–767, 2015.

[43] Ting-ting Zhu, He Wang, Pan-miao Liu, Han-wen Gu, Wei-tong Pan, Ming-ming Zhao, Kenji Hashimoto, and Jian-jun Yang. Clemastine-induced enhancement of hippocampal myelination alleviates memory impairment in mice with chronic pain. *Neurobiology of Disease*, 190:106375, 2024.

[44] Francesco Brigo, Eugen Trinka, Simona Lattanzi, Nicola Luigi Bragazzi, Raffaele Nardone, and Mariano Martini. A brief history of typical absence seizures—petit mal revisited. *Epilepsy & Behavior*, 80:346–353, 2018.

[45] Damien Depannemaecker, Aitakin Ezzati, Huifang Wang, Viktor Jirsa, and Christophe Bernard. From phenomenological to biophysical models of seizures. *Neurobiology of Disease*, page 106131, 2023.

[46] Hugh R Wilson and Jack D Cowan. Excitatory and inhibitory interactions in localized populations of model neurons. *Biophysical journal*, 12(1):1–24, 1972.

[47] Jack D Cowan, Jeremy Neuman, and Wim van Drongelen. Wilson–cowan equations for neocortical dynamics. *The Journal of Mathematical Neuroscience*, 6(1):1–24, 2016.

[48] Gustavo Deco, Viktor K Jirsa, Peter A Robinson, Michael Breakspear, and Karl Friston. The dynamic brain: from spiking neurons to neural masses and cortical fields. *PLoS computational biology*, 4(8):e1000092, 2008.

[49] Edward G Jones. Microcolumns in the cerebral cortex. *Proceedings of the National Academy of Sciences*, 97(10):5019–5021, 2000.

[50] Scott Rich, Axel Hutt, Frances K Skinner, Taufik A Valiante, and Jérémie Lefebvre. Neurostimulation stabilizes spiking neural networks by disrupting seizure-like oscillatory transitions. *Scientific reports*, 10(1):15408, 2020.

[51] Maria Luisa Saggio, Dakota Crisp, Jared M Scott, Philippa Karoly, Levin Kuhlmann, Mitsuyoshi Nakatani, Tomohiko Murai, Matthias Dümpelmann, Andreas Schulze-Bonhage, Akio Ikeda, et al. A taxonomy of seizure dynamotypes. *Elife*, 9:e55632, 2020.

[52] Mark O Cunningham, Anita Roopun, Ian S Schofield, Roger G Whittaker, Roderick Duncan, Aline Russell, Alistair Jenkins, Claire Nicholson, Miles A Whittington, and Roger D Traub. Glissandi: transient fast electrocorticographic oscillations of steadily increasing frequency, explained by temporally increasing gap junction conductance. *Epilepsia*, 53(7):1205–1214, 2012.

[53] Kristina D Micheva, Marianna Kiraly, Marc M Perez, and Daniel V Madison. Conduction velocity along the local axons of parvalbumin interneurons correlates with the degree of axonal myelination. *Cerebral Cortex*, 31(7):3374–3392, 2021.

[54] Minghui Zhu, Weiwei Liu, and Pawel Wargocki. Changes in eeg signals during the cognitive activity at varying air temperature and relative humidity. *Journal of exposure science & environmental epidemiology*, 30(2):285–298, 2020.

[55] Odin Dumas. My analysis notebook. `https://colab.research.google.com/drive/1fOL-woi3UGm6TIS-jk61_79flKlDZ9dZ?usp=sharing/<link>`, 2024. Accessed: date.

[56] Andre Longtin. Neuronal noise. *Scholarpedia*, 8(9):1618, 2013.

[57] John J Hopfield. Neurons with graded response have collective computational properties like those of two-state neurons. *Proceedings of the national academy of sciences*, 81(10):3088–3092, 1984.

[58] Gonzalo Alarcon, CD Binnie, RDC Elwes, and CE Polkey. Power spectrum and intracranial eeg patterns at seizure onset in partial epilepsy. *Electroencephalography and clinical neurophysiology*, 94(5):326–337, 1995.

[59] Maher A Quraan, Cornelia McCormick, Melanie Cohn, Taufik A Valiante, and Mary Pat McAndrews. Altered resting state brain dynamics in temporal lobe epilepsy can be observed in spectral power, functional connectivity and graph theory metrics. *PloS one*, 8(7):e68609, 2013.

[60] Kaveh Samiee, Peter Kovacs, and Moncef Gabbouj. Epileptic seizure classification of eeg time-series using rational discrete short-time fourier transform. *IEEE transactions on Biomedical Engineering*, 62(2):541–552, 2014.

[61] Ronald N Bracewell. The fourier transform. *Scientific American*, 260(6):86–95, 1989.

[62] Christopher Bingham, Michael Godfrey, and John Tukey. Modern techniques of power spectrum estimation. *IEEE Transactions on audio and electroacoustics*, 15(2):56–66, 1967.

[63] Jorge F Mejias and André Longtin. Differential effects of excitatory and inhibitory heterogeneity on the gain and asynchronous state of sparse cortical networks. *Frontiers in computational neuroscience*, 8:107, 2014.

[64] Mark S Cembrowski and Nelson Spruston. Heterogeneity within classical cell types is the rule: lessons from hippocampal pyramidal neurons. *Nature Reviews Neuroscience*, 20(4):193–204, 2019.

[65] Homeira Moradi Chameh, Scott Rich, Lihua Wang, Fu-Der Chen, Liang Zhang, Peter L Carlen, Shreejoy J Tripathy, and Taufik A Valiante. Diversity amongst human cortical pyramidal neurons revealed via their sag currents and frequency preferences. *Nature communications*, 12(1):2497, 2021.

[66] Esther Krook-Magnuson, Csaba Varga, Sang-Hun Lee, and Ivan Soltesz. New dimensions of interneuronal specialization unmasked by principal cell heterogeneity. *Trends in neurosciences*, 35(3):175–184, 2012.

[67] Greg A Worrell, Landi Parish, Stephen D Cranstoun, Rachel Jonas, Gordon Baltuch, and Brian Litt. High-frequency oscillations and seizure generation in neocortical epilepsy. *Brain*, 127(7):1496–1506, 2004.

[68] Carlo Laing and Stephen Coombes. The importance of different timings of excitatory and inhibitory pathways in neural field models. *Network: Computation in Neural Systems*, 17(2):151–172, 2006.

[69] Axel Hutt and Fatihcan M Atay. Analysis of nonlocal neural fields for both general and gamma-distributed connectivities. *Physica D: Nonlinear Phenomena*, 203(1-2):30–54, 2005.

[70] Patricia E Penovich, Janice Buelow, Kathy Steinberg, Joseph Sirven, and James Wheless. Burden of seizure clusters on patients with epilepsy and caregivers. *The neurologist*, 22(6):207–214, 2017.

[71] Gretchen L Birbeck, Ron D Hays, Xinping Cui, and Barbara G Vickrey. Seizure reduction and quality of life improvements in people with epilepsy. *Epilepsia*, 43(5):535–538, 2002.

[72] A Ulate-Campos, F Coughlin, M Gaínza-Lein, I Sánchez Fernández, PL Pearl, and T Loddenkemper. Automated seizure detection systems and their effectiveness for each type of seizure. *Seizure*, 40:88–101, 2016.

[73] Ivan W Selesnick and C Sidney Burrus. Generalized digital butterworth filter design. *IEEE Transactions on signal processing*, 46(6):1688–1694, 1998.

[74] Shennan Aibel Weiss, Catalina Alvarado-Rojas, Anatol Bragin, Eric Behnke, Tony Fields, Itzhak Fried, Jerome Engel Jr, and Richard Staba. Ictal onset patterns of local field potentials, high frequency oscillations, and unit activity in human mesial temporal lobe epilepsy. *Epilepsia*, 57(1):111–121, 2016.

[75] Harvey A Swadlow and Stephen G Waxman. Axonal conduction delays. *Scholarpedia*, 7(6):1451, 2012.

[76] Kelin Li, Xinhua Zhang, and Zuoan Li. Global exponential stability of impulsive cellular neural networks with time-varying and distributed delay. *Chaos, Solitons & Fractals*, 41(3):1427–1434, 2009.

[77] Houman Khosravani and Gerald W Zamponi. Voltage-gated calcium channels and idiopathic generalized epilepsies. *Physiological reviews*, 86(3):941–966, 2006.

[78] P Michelle Fogerson and John R Huguenard. Tapping the brakes: cellular and synaptic mechanisms that regulate thalamic oscillations. *Neuron*, 92(4):687–704, 2016.

[79] Luis F Lopez-Santiago, Yukun Yuan, Jacy L Wagnon, Jacob M Hull, Chad R Frasier, Heather A O'Malley, Miriam H Meisler, and Lori L Isom. Neuronal hyperexcitability in a mouse model of scn8a epileptic encephalopathy. *Proceedings of the National Academy of Sciences*, 114(9):2383–2388, 2017.

[80] J Musgrave and P Gloor. The role of the corpus callosum in bilateral interhemispheric synchrony of spike and wave discharge in feline generalized penicillin epilepsy. *Epilepsia*, 21(4):369–378, 1980.

[81] Yue Liu, John Milton, and Sue Ann Campbell. Outgrowing seizures in childhood absence epilepsy: time delays and bistability. *Journal of Computational Neuroscience*, 46:197–209, 2019.

[82] John G Milton, André Longtin, Anne Beuter, Michael C Mackey, and Leon Glass. Complex dynamics and bifurcations in neurology. *Journal of theoretical biology*, 138(2):129–147, 1989.

[83] Kyle CA Wedgwood, Kevin K Lin, Ruediger Thul, and Stephen Coombes. Phase-amplitude descriptions of neural oscillator models. *The Journal of Mathematical Neuroscience*, 3:1–22, 2013.

[84] Peter J Hand and Adrian R Morrison. Thalamocortical projections from the ventrobasal complex to somatic sensory areas i and ii. *Experimental neurology*, 26(2):291–308, 1970.

[85] EG Jones and DP Friedman. Projection pattern of functional components of thalamic ventrobasal complex on monkey somatosensory cortex. *Journal of neurophysiology*, 48(2):521–544, 1982.

[86] Gustavo Chau Loo Kung, Juliet K Knowles, Ankita Batra, Lijun Ni, Jarrett Rosenberg, and Jennifer A McNab. Quantitative mri reveals widespread, network-specific myelination change during generalized epilepsy progression. *Neuroimage*, 280:120312, 2023.

[87] Bruce Hutcheon and Yosef Yarom. Resonance, oscillation and the intrinsic frequency preferences of neurons. *Trends in neurosciences*, 23(5):216–222, 2000.

[88] Aneta Stefanovska and Peter VE McClintock. *Physics of Biological Oscillators*. Springer, 2020.

[89] Gerd Gigerenzer. What are natural frequencies? *Bmj*, 343, 2011.

[90] Natalia Dabrowska, Suchitra Joshi, John Williamson, Ewa Lewczuk, Yanhong Lu, Samrath Oberoi, Anastasia Brodovskaya, and Jaideep Kapur. Parallel pathways of seizure generalization. *Brain*, 142(8):2336–2351, 2019.

[91] Ali A Asadi-Pooya, Ashwini Sharan, Maromi Nei, and Michael R Sperling. Corpus callosotomy. *Epilepsy & Behavior*, 13(2):271–278, 2008.

[92] Kenneth L Davis, Daniel G Stewart, Joseph I Friedman, Monte Buchsbaum, Philip D Harvey, Patrick R Hof, Joseph Buxbaum, and Vahram Haroutunian. White matter changes in schizophrenia: evidence for myelin-related dysfunction. *Archives of general psychiatry*, 60(5):443–456, 2003.

[93] Douglas C Dean, Samuel A Hurley, Steven R Kecskemeti, J Patrick O'Grady, Cristybelle Canda, Nancy J Davenport-Sis, Cynthia M Carlsson, Henrik Zetterberg, Kaj Blennow, Sanjay Asthana, et al. Association of amyloid pathology with myelin alteration in preclinical alzheimer disease. *JAMA neurology*, 74(1):41–49, 2017.

[94] Maria Podbielska, Naren L Banik, Ewa Kurowska, and Edward L Hogan. Myelin recovery in multiple sclerosis: the challenge of remyelination. *Brain sciences*, 3(3):1282–1324, 2013.